Transactions of the I·R·E

Professional Group on Antennas and Propagation

JOINT URSI - IRE MEETING

Cornell University, Ithaca, New York

October 8-10, 1951

Papers sponsored by

Commissions 2 and 3 of the USA National Committee

of the International Scientific Radio Union

and the

IRE Professional Group on Antennas and Propagation

Price per copy—

Members of the IRE Professional Group on Antennas and Propagation—$1.50

Members of the IRE—$2.25

Nonmembers—$4.50

Lithoprinted in the United States of America

PGAP—2

MARCH, 1952

The Institute of Radio Engineers

TRANSACTIONS of the I.R.E.

Professional Group on Antennas and Propagation

PGAP - 2 March, 1952

TABLE OF CONTENTS

Commission 2, Tropospheric Radio Propagation

Commission 3, Ionospheric Radio Propagation

TRANSACTIONS of the I.R.E.

Professional Group on Antennas and Propagation

PGAP - 2 March, 1952

TABLE OF CONTENTS

THE ROLE OF PARTIAL REFLECTIONS IN TROPOSPHERIC PROPAGATION BEYOND THE HORIZON

J. Feinstein
National Bureau of Standards
Washington, D.C.

1. Introduction

Measurements on vhf transmissions in recent years have indicated that field strengths deep in the diffraction region are many orders of magnitude greater than values calculated on a smooth earth diffraction theory, even when allowance is made for the refraction produced by the standard atmosphere.[1] Of the theories advanced to date in explanation of this effect, the machanism of scattering by inhomogeneities resulting from atmospheric turbulence has perhaps been the most successful.[2] However, certain discrepancies in wavelength and angle dependence, together with the fact that the abnormal fields apparently exist everywhere at all times, lead one to seek an explanation solely in terms of the model represented by the standard atmosphere.

2. Partial Reflection Calculations

It is well known that a discontinuity in the characteristics of a medium traversed by a wave gives rise to a reflected as well as a transmitted wave. Such reflections have been invoked in explanation of certain tropospheric effects.[3] Bremmer[4] has recently stressed the fact that a gradual change in medium properties produces the same effect in principle, although the magnitude of the continuously reflected components is then generally quite small. Since the atmosphere possesses a gradient of refractive index, such partial reflections must occur. By this mechanism it appears that wave energy may be delivered to areas far beyond the line of sight of the transmitter. Since the diffracted field decays exponentially with distance in this region, while the reflections diminish only as an inverse power of the distance, the latter dominate rather rapidly.

While it should, of course, be possible to obtain these

reflections from a rigorous wave formulation of the problem of a dipole in an inhomogeneous atmosphere above a spherical earth, the sought-for modification of the standard mode theory has thus far not been found. We shall return to this question later, but at present it appears feasible to estimate the magnitude of the field produced by means of a hybrid ray and wave theory along the following lines:[5] as shown in Fig. 1, the contributions to the field at any receiving point will come from those partial reflections originating in areas for which the equal angle law of specular reflection is satisfied. When transmitter and receiver are on the surface of the earth, this locus is the perpendicular bisector of the line connecting them. Across any differential distance dh along this locus, we consider the beam incident upon the troposphere to be a plane wave whose angle of incidence α with respect to the spherical stratification is a function of the geometry and of atmospheric refraction. If, further, we replace the spherical surfaces of constant refractive index by plane stratification, and take account of the convergent effect upon the wavefront through a coefficient $C(\alpha)$, then it may be shown[4] that the differential reflection is

$$\frac{K dh}{2\alpha^2} C(\alpha), \qquad \text{where} \qquad K = \frac{dn}{dh},$$

the gradient of refractive index. Adding the contributions all along h with their proper phase,

$$R = \int_{h(\alpha_o)}^{\infty} \frac{K(\alpha)}{2\alpha^2} \exp(ikh\alpha) \cdot f_T(\alpha) \cdot f_R(\alpha) \cdot C(\alpha) \cdot dh \qquad (1)$$

where the f functions are the effective antenna patterns; α_o is the minimum angle of incidence possible, corresponding to a ray leaving the earth at a grazing angle. For the hypothetical case of antenna patterns isotropic beyond a given angle α_1 and a uniform gradient, an asymtotic series may be obtained for (1), of which the leading term is:

$$R \simeq \frac{K}{4 k\beta^3} \qquad (2)$$

where $\beta = \alpha_o + \alpha_1$.

This is valid for $\frac{1}{kD\beta^2} \ll 1$, where D is the half-distance between horizon points of transmitter and receiver antennas.

In agreement with our physical ideas, the magnitude of the reflection depends upon K/k, the change in the medium properties per wavelength.

Results calculated from this formula are plotted in Fig. 2, for the gradient associated with the standard atmosphere. The departure from linearity at long distances is caused by the exponential decline in K at great heights.

A more practical type antenna consists of a dipole above a perfectly conducting earth, giving rise to a lobe structure in the radiation pattern; (1) then takes the form

$$R = \frac{KD}{2} \int_{\alpha_0}^{\pi/2} \frac{e^{ikD\alpha^2}}{\alpha^2} \sin kh_1 (\alpha - \alpha_0) \sin kh_2 (\alpha - \alpha_0) \, d\alpha . \qquad (3)$$

The gradient K has been taken as constant here, and is to be given the value $K(\alpha_0)$.

The convergence factor has been neglected here, since its effect is small beyond the tangent ray, and it is doubtful whether phase coherence exists over a sufficiently large region to yield the theoretical gain for the latter. As before, D is the half distance between horizon points of transmitter and receiver antennas; $h_{1,2}$ are related to the physical antenna heights, $H_{1,2}$ by

$$h = H \left[\frac{D}{D + \sqrt{2a_e H}} \right] \qquad (4)$$

where a_e is the effective earth's radius.

The evaluation of (3) proceeds by expanding the trigonometric functions and making appropriate substitutions so as to obtain several integrals of the form:

$$\int e^{ikDx} \frac{\begin{matrix}\sin \\ \cos\end{matrix} s\sqrt{x}}{x^{3/2}} \, dx . \qquad (5)$$

These may be evaluated by parts to yield asymptotic series,

similar to that leading to (2). One obtains

$$R \simeq \frac{K}{4k\alpha_o^5} \cdot \frac{h_1}{D} \cdot \frac{h_2}{D} \tag{6}$$

if $$\frac{1}{kD\alpha_o^2} \ll 1 \quad \text{and} \quad \frac{h_{1,2}}{\alpha_o D} \ll 1 \ . \tag{7}$$

In addition, since (6) is obtained from an asymptotic series, the left-hand sides of (7) give a measure of the error incurred. Since $\alpha_o = \frac{D}{a_e}$, (6) will generally be an adequate approximation, except for very high antennas

$$(h \simeq D^2/a_e) \tag{8}$$

In this event, which corresponds to a single lobe of the radiation pattern falling within a Fresnel zone at the reflecting region, the isotropic case is approached. Mathematically, this corresponds to a removal from (6) of a factor $\frac{h}{\alpha_o D}$ for each antenna satisfying (8).

Further increase in antenna height will result in a diminution of received signal as a result of the cancellation within a single Fresnel zone produced by the phase reversal in successive lobes.

As a consequence of the specular nature of the reflection, the angular characteristics of the received signal will be similar to those obtained with both antennas on a plane earth.

3. The Reconciliation Problem

The mode theory of wave propagation due to a dipole over a spherical earth is a rigorous wave approach to the problem. By utilizing separation of variables in the radical and angular co-ordinates, a series solution is obtained in which the eigenvalues of a radical wave equation appear in the exponential factor governing the distance dependence. Since these

eigenvalues are generally complex,[6] an exponential attenuation is obtained. In the evaluation of the radical wave functions, a WKB type approximation, or one equivalent to it, is generally employed. Since it is well known that in the case of infinite plane waves WKB solutions represent traveling waves for which the loss in intensity occasioned by the continuous partial reflections is taken into account, while the new waves arising from these reflections are entirely neglected, it would appear that the resolution of the dilemma is apparent. Further study, however, fails to bear this out. In the mode treatment, the wave functions in question are employed only to obtain values of their index for which the functions themselves, or their derivatives, vanish. The slight correction represented by the terms neglected in the WKB method do not appear to affect these index values materially. Furthermore, precisely the same type of approximation is employed in the homogeneous atmosphere calculation as for an inhomogeneous atmosphere obeying a refractive index law of the form $k^2(r) = A + B/r^2$. As is well known[7], the modification introduced by the inhomogeneity may be expressed in terms of an equivalent earth radius which is purely a function of the dielectric gradient at the earth's surface. Physically, it is apparent that this takes account of refraction, but the partial reflections which would be expected to accompany this refraction do not appear to be present. It should be noted that the physical nature of these two inverse radius squared terms which appear in the radical wave equation

$$\nabla_r^2 \psi + k^2(r) - \frac{n(n+1)}{r^2}\psi = 0 \qquad (9)$$

with

$$k^2(r) = A + \frac{B}{r^2} \qquad (10)$$

is distinct. In a homogeneous atmosphere this type of dependence arises when one expresses radiation traveling in straight line rays in a curvilinear co-ordinate system; on the other hand the B/r^2 corresponding to the inhomogeneous atmosphere is responsible for a true bending of the rays. Thus the interpretation of the WKB approximation given by Bremmer[8], for example, would appear to apply only to this second type of variation. Furthermore, since partial reflection of the energy in a ray bundle only accompanies true bending of the ray, the preservation of relative curvature which forms the basis for the various earth flattening approximations can be valid only when the partial reflections introduced by the supposedly equivalent refractive index profile are negligible.

In the region above the horizon, the field is generally found by applying stationary phase methods to the contour integral representation in which WKB approximations to the wave functions have been employed. This procedure yields the direct and earth-reflected rays only. Now the sum of modes which is employed to represent the field in the shadow region may be obtained by extending the concept of stationary phase to include complex angles.[9] Since the same (WKB) approximations are employed in this evaluation, one feels justified in drawing the conclusion that partial reflections have been neglected in the usual mode series representation, just as they are neglected by the two-ray treatment above the horizon. Furthermore, since the introduction of a second term in the wave function approximation would give rise to the sought-for additional paths of stationary phase above the horizon[10], it is logical to assume that in the shadow region the partial reflections will be represented by additional modes arising from the higher order approximation. While these modes will be only weakly excited compared to the standard first order modes, their characteristic values will be such as to give rise to far less distance attenuation.

Since it has not proved possible to carry through this program up to the present, the above discussion is mainly speculative. Consequently the treatment given in section 2 must be viewed with caution, especially as regards the quantitative results which are given.

References

1. "Radio Progress in 1950", Proc. I.R.E., vol. 39, p. 391; 1951.

2. H.G. Booker and W.E. Gordon, Proc. I.R.E., vol. 38, p. 401; 1950.

3. K.A. Norton, "Advances in Electronics", vol. 1, p. 402 et seq.; 1948.

4. H. Bremmer, Philps Res. Rep., vol. 4, p. 1; 1949; Physica, vol. 15, p. 593; 1949.

5. J. Feinstein, Jour. Appl. Phys., vol. 22, p. 1292; 1951.

6. A. Sommerfield, "Partial Differential Equations", p. 214 et seq.; 1949.

7. M.I. Ponomarev, Bull. Acad. Sci., (U.S.S.R.), vol. 9, p. 219; 1946.

8. H. Bremmer, "Terrestrial Radio Waves", Elsevier Publishing Co., p. 158; 1949.

9. C.L. Pekeris, Jour. Appl. Phys.; 1948.

10. H. Bremmer, Physics, vol. 15, p. 605; 1949.

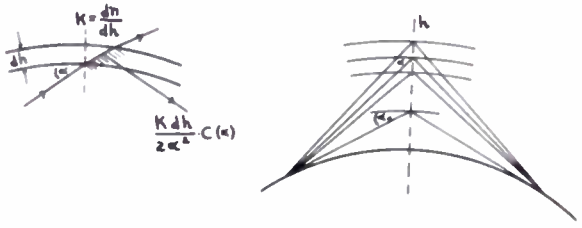

Fig. 1

Schematic representation of partial reflections

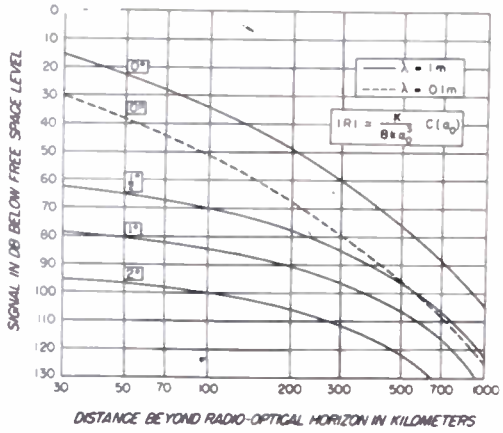

Fig. 2

Signal level as a function of distance for antenna patterns isotropic beyond the angle α_1 indicated on the curves

INTERNAL REFLECTION IN THE TROPOSPHERE AND PROPAGATION BEYOND THE HORIZON

Thomas J. Carroll
National Bureau of Standards
Washington, D.C.

I. INTRODUCTION

Since the last year of World War II, the outstanding problem in tropospheric propagation research has been the explanation of the high observed field strengths well beyond the horizons of high-power transmitters, at all frequencies throughout the vhf and microwave spectrum, in widely separated parts of the world under vastly different conditions of climate and terrain. The disagreement between measurements and calculations based on conventional theory of propagation over a smooth earth surmounted by an atmosphere with standard refraction (4/3 earth) has become steadily worse as the powers and distances have increased, so that the term "discrepancy" seems like a considerable understatement, 40 db and more discrepancies of median observed fields above the conventionally calculated value being not at all uncommon beyond 100 miles. Discussion and references appear in recent annual progress reviews on tropospheric propagation. [1, 2, 3]

The leading hypotheses heretofore suggested for bridging this embarrassing gap between measurement and theory have been (a) scattering by atmospheric turbulence (Pekeris, Booker and Gordon,[4] and others), and (b) scattering associated with roughness of the earth's surface (Bullington[5]). Recently Feinstein[6,7] has published a suggestion that partial reflections from the normal troposphere may be part of the explanation. It is the purpose of this paper to outline an alternative method of estimating the magnitude of partial internal reflections from the troposphere well beyond the horizon, following the method of Feinstein and Bremmer[8]; to show how well this formulation agrees with the data examined so far mostly at 50 mc and 3,000 mc, and to indicate why the conventional wave theory for standard refraction may not be applied too far beyond the horizon.

2. The Physical Idea

The fundamental physical notion concerning internal reflection from the normal troposphere may be expressed as follows, following Bremmer and Feinstein: At a plane horizontal interface at some height above the earth, let the index of refraction

below be n, and that above be n-dn (fig. 1). If a plane wave strikes the interface from below at a glancing angle α, then in addition to a transmitted wave above, moving by Snell's law somewhat more horizontally, there will also be below the interface a weak reflected wave traveling downward at the same glancing angle α internal to the medium where the incident wave was traveling. The magnitude of the infinitesimal reflection coefficient (field strength) dR is $dn/2\alpha^2$, for small glancing angles. A quite general derivation by Bremmer[8] is given for the "scattering coefficient per unit thickness" of a plane stratified medium in the z direction, for plane waves, namely,

$$\frac{1}{2}\frac{d}{dz}\log\frac{(\sin\alpha)}{(n)}.$$

For small glancing angles, Bremmer's formula reduces to $dn/2\alpha^2$, and for normal incidence to the well-known $dn/2$. (It should perhaps be noted that if the interface be enlarged to a finite layer through which the index decreases continuously by a total amount Δn, then the layer as a whole will totally reflect below the layer back into the medium of greater index all waves with glancing angle less than the critical value $\alpha_o = \sqrt{2\Delta n}$, independently of the precise law of decrease of index in the layer.) For interfaces at which only infinitesimal changes occur, as well as for layers of finite thickness at glancing angles greater than critical, the internal reflection is only partial, of course. At glancing angles greater than critical, the partial reflections for a finite layer are wavelength dependent, because destructive interference effects set in as soon as the path difference between reflections from the top and bottom of the layer exceed a half wavelength. (See for example the tables of Millington in [9] calculated for linearly graded layers.)

The term "internal reflection" is used here following the authors Eckart and Kahan[10] who have calculated this effect at normal incidence, and use the terms "internal" and "external", respectively, to distinguish between the reflections from a continuously graded medium, and the reflection at a discontinuity of index. In optics the term "total internal reflection" is usually applied to describe reflection in the medium of greater index at an angle of incidence greater than critical. Perhaps it would be desireable to use the term "partial internal reflection" when it is desired to emphasize the nontotality or the weakness of the reflection. Friend, on the other hand, also calculating the reflection effect in a linearly graded medium at vertical incidence, uses no qualifying adjectives before "reflection coefficient".

It is contended in this paper that the entire difficulty with conventional theory applied too far beyond the horizon for the normal troposphere arises from the neglect of the weak,

though omnipresent reflected waves of Fig. 1 at large distances beyond the horizon, for which the glancing angles on the normal troposphere are sufficiently small to make the effect nonnegligible.

Fig. 2 shows a diagram of the earth bulge between two well separated transmitting and receiving points T and R, a distance D = 2d apart. (D is negligibly different in what follows from the distance as measured along the surface.) Because it is believed necessary to take the lobe structure explicitly into account from the beginning, the distance is measured between the transmitting and receiving locations themselves. α_o is the elevation angle of the earth's surface at each location from the line joining the transmitting and receiving locations on the surface of the idealized earth. Along a vertical line over the middle of the path, the normal troposphere is idealized as a plane stratified medium with index decreasing by $1.2(10)^{-8}$ per foot near the surface, which will reflect radiation from T to R, according to the equal angle law, from each slice of the atmosphere in which the index decreases with height. If z is the height of a reflection point Q at angle of elevation α over the middle of the path, then the path difference

$$TQR-TR \cong \frac{z^2}{d} \cong \alpha z \cong d\alpha^2.$$

The corresponding phase difference is $kd\alpha^2$, where $k = \frac{2\pi}{\lambda}$.

Adding up the partial internal reflections over all layers from the surface z_o up to great heights, a formula very similar to Feinstein's equation (1)[6] results, namely

$$R = \frac{E_r}{E_{fs}} \int_{z_o}^{\infty} \frac{dn}{2\alpha^2} \exp\left(ikd\alpha^2\right) f_T(\alpha) f_R(\alpha) \qquad (1)$$

where E_r is the resultant internally reflected field from the troposphere, and E_{fs} is the free space field at the distance 2d. The first factor in the integrand gives the plane wave reflection coefficient for a layer of index change dn for a plane wave at glancing angle α. The second factor is the phase factor giving the phase delay of higher layers relative to lower layers, and the last two factors give the transmitting and receiving antenna patterns, including the lobes resulting from surface reflections in the neighborhoods of T and R. Two lobes of the vertical pattern of the transmitting and receiving antennas are sketched in Fig. 2.

For a deeper insight into the validity of (1), the reader should study the portion of Bremmer's paper (section 7 of [8]) leading up to (23), where a more thorough treatment is given.

Bremmer describes the process of obtaining (1), for dipole antennas, and neglecting the earth, as a decomposition of the outgoing radiation into plane waves at various angles, the production of new plane waves by the plane stratified medium (in this application the troposphere over the middle of the path), and the combination of these waves at the receiving antenna. The only physical approximation in (1) is the neglect of convergence or divergence factors by treating the normally stratified troposphere as if it were plane over the middle of the path.

3. Estimating The Integral

(a) Wave Length Dependence and Lobes[26]

All Feinstein's published approximations[6,7] to the integral (1) implied that the tropospherically reflected fields were proportional to the wavelength λ, in apparent contradiction with observations on wavelength dependence of tropospheric scattering at S,X, and K bands by the NEL group, and seemed also to imply too rapid a decrease in going from vhf to microwaves. (This λ factor arises from the phase factor of the integral, because the first factor, the reflection coefficient, is independent of frequency. Two points, S and Q on the vertical at midpath, define what may be called a Fresnel half-wave layer of the troposphere if TQR exceeds TSR by $\frac{\lambda}{2}$. Such a height increase changes the phase factor in (1) by π, and this thickness QS will be the maximum for which the reflections can add together without destructive interference. As shown to the left of Fig. 2, the Fresnel half-wave layer thickness well above TR is $\frac{\lambda}{4\alpha}$.) If the most important part of the reflection be considered to be that near the lobe maximum rather than just above the horizon, then a compensating factor favoring microwaves over vhf seems to enter. The angles of elevation of the interference lobes which were so thoroughly explored experimentally during the war in connection with radar coverage patterns, depend essentially on the height of the antenna in wavelengths above the reflecting earth. The main contribution to the integral (1) comes from layers where the glancing angle α can be made small enough in the denominator to compensate for the smallness of the index lap rate ($1.2(10)^{-8}$ per foot in the normally stratified troposphere), and still are favorably situated with respect to the antenna patterns. These physical arguments almost force the conclusion that the main contribution to the integral comes from the tropospheric layers at mid path, above the horizon of each antenna and below the lowest lobe maximum of the lower antenna. Thus it was reasoned that the low angles of the lobes for higher frequencies with result-

ing smaller glancing angles against the troposphere stratifications could compensate partly or completely for the smaller thickness of a half-wavelayer for the higher frequencies.

The integral (1) containing only the exponential factor would be a Fresnel integral, familiar in diffraction problems, and the result would trace out a Cornu spiral in the complex plane. The factor $\frac{f_T f_R}{\alpha^2}$ serves as a modulating factor, so that the integral and its graphical representation could well be called a modulated Fresnel integral or a pulsating Cornu-like spiral. Because the successive half-wave layers make contributions of opposite sign to the total result, the familiar Fresnel-like arguments of optics have been employed to estimate that the total result may be of the order of magnitude of 1/2 the reflected field from the half-wave layer of maximum contribution. These arguments will be outlined in section 5 below. Accepting this, the estimate of the integral becomes

$$R = 1/2 \left[\frac{2}{\pi}\frac{\lambda K}{4\alpha}\frac{f_T(\alpha)}{2\alpha^2}\frac{f_R(\alpha)}{}\right]_{max} = \left[\frac{K\lambda}{8\pi}\frac{f_T(\alpha)}{\alpha^3}\frac{f_R(\alpha)}{}\right]_{max} \qquad (2)$$

where $K \cong \frac{dn}{dh}$, assumed constant over a particular half-wave layer. When the maximum layer occurs at great heights, the value of K decreases exponentially with height in the upper troposphere (see section 6 below).

(b) Special Cases

Several special cases of (2) have been used in comparing the formula with measurements. On Fig. 2, α_T is the angle of elevation of the lowest transmitter lobe above the ground, approximately $\frac{\lambda}{4h_T}$ where h_T is the transmitting antenna height. The general expression (2) leads to simple approximations in several special cases where it becomes easy to estimate at what α the maximum of the square bracket expression occurs.

Case a. Long Distance, Low Lobes (Equal Antenna Heights)

If the distance is sufficiently long that α_o is much bigger than $\alpha_T = \alpha_R$, then the maximum contribution will occur practically at the level in the atmosphere where the lowest lobes maxima intersect at mid path, and the value of $f_T = f_R = 2$ may used, corresponding to twice the free space value of the field strength obtained at lobe maxima, and $\alpha_{max} = \alpha_o + \alpha_T$, giving

$$R = \frac{K\lambda}{2\pi(\alpha_{max})^3} = \frac{K\lambda}{2\pi(\alpha_o + \alpha_T)^3} \qquad (3)$$

Case b. Long Range, One Antenna Low, Giving High Lobes

In this case, the pattern factor f in (2) for the "high" antenna may be put equal to 2, but for the "low" antenna (α_T or $\alpha_R \gg \alpha_o$), the maximum of $\left(\frac{f}{\alpha^3}\right)_{max}$ must be computed separately. Putting f zero below the horizon and using the simple flat earth approximation above, namely $f = 2 \sin kh(\alpha-\alpha_o)$, the maximum of $\frac{f}{\alpha^3}$ occurs at $\alpha_{max} = \frac{3}{2}\alpha$ and

$$R = \frac{K\lambda}{27\alpha_o^2\alpha_R} \qquad (4)$$

If for α_R, the angle of elevation of the lowest lobe of the receiving antenna above the horizontal we put $\frac{\lambda}{4h_R}$, then (4) becomes

$$R = \frac{4\,(Kh)}{27\,\alpha_o^2} . \qquad (4a)$$

In this approximation, it may be noted that the wavelength has disappeared; in other words the high angle of the lowest lobe of the low antenna discriminates against the lower frequencies so as to cancel exactly (in this approximation) the advantage the lower frequencies have because a half-wave layer thickness is proportional to the wavelength.

Case c. Both Antenna Heights Low and Equal

By "low" is meant $\alpha_R = \alpha_T \gg \alpha_o$, i.e., high lobes compared to the angle α_o determined by the earth bulge. If both the antenna pattern functions f are approximated as zero below the horizon and 2 sin k h $(\alpha - \alpha_o)$ above, then the maximum value of the square bracket in (2) can be shown to occur at $\alpha_{max} = 3\alpha_o$, and the value of R becomes

$$R = \frac{K\pi\lambda}{54\,\alpha_R^2\,\alpha_o} . \qquad (5)$$

If the lobe angle α_R is put equal to $\frac{\lambda}{4h}$, this becomes

$$R = \frac{8\,K\,\pi\,h^2}{27\,\lambda\,\alpha_o} . \qquad (5a)$$

Note that the wavelength appears in the denominator of this expression.

It is possible that such a formula as (5a) may afford an explanation of Smyth's observation of the experimental wavelength dependence of scattered fields. "A comparison of the 3-cm and 10-cm signals relative to their expected free-space values proved the shorter wavelength field to be some 10 to 12 db higher in level than the 10-cm radiation" (p. 93 of [15]). Detailed comparison of (5a) with Smyth's data has not yet been completed because it is not yet known whether the antenna heights of the data to which Smyth's remarks refer qualify as being "low" in the snese of case c.

4. Comparison With Measurements

a. Lower vhf Frequencies

It is important to emphasize that applied to the normal atmosphere, the above formulas have no adjustable parameters whatever, and are subject only to certain mathematical and physical approximations which will be discussed in the next section. The most powerful evidence at the present time for believing the essential truth of this explanation of distant tropospheric fields is the remarkable order of magnitude agreement with data which has long been a puzzle. Fig. 3 shows agreement with data in the 40- to 50-mc band. Each of the points represents the average field strength over a recording period of six months to a year. All but one of the points are the same as those shown by Bullington in his paper of January, 1950[12]. The only additional point is the RCA data at 66 miles, taken from item 43 in [12a]. All the data are reduced in the manner described by Bullington so that they refer to transmitting antenna height of 500 feet, and receiving antenna height of 30 feet. The two lower curves are drawn beyond line of sight for conventional single mode diffraction theory, using geometrical earth radius, and 4/3 earth radius to correct for normal refraction. Finally, there is plotted the curve marked "Internal Reflection" from (4a) at the larger ranges where it lies above the 4/3 earth curve. (Strictly speaking, this curve should be labeled "Half the reflected field from the half-wave layer of maximum contribution.") Only order of magnitude agreement is to be expected because the points represent averages over many months of fluctuating non-optical fields which fade by many tens of decibels over long and short periods. The improvement of the internal reflection curve in explaining the average fields beyond about 100 miles compared to the 4/3 earth curve is apparent.

b. Microwaves

The other data to which quantitative curves have been com-

pared is shown on Fig. 4, for 3,000 mc. The solid points represent data published by Megaw[13]. He describes these as representing the average data obtained on six runs across the North Sea during a six-week period during the summer of 1949, after all data were thrown out for periods when superrefraction was thought to be present, as judged by meteorological data or the radio records. Megaw states that 90 per cent of all the observations used lay within ± 5 db of the plotted points. The square points on Fig. 4 represent Megaw's estimate of Katzin's Carribean observation of 1945, for conditions of negligible superrefraction. Confirmation of the slope of these experimental curves has also been reported by Katzin from later measurements in the Pacific [14]. Unfortunately, Megaw did not publish the antenna heights to which his observations refer. He interpreted his points in terms of his new theory of scattering from atmospheric turbulence. The curve marked "internal reflection" has been computed using assumed antenna heights of 100 feet. (Somewhat more refined formulas than those of the preceding section were used for this curve, corresponding to the well-known but tedious complication in lobe calculations that when the lowest lobe lies close to the horizon, the effective reflecting plane becomes the tangent to the reflecting point, and the effective height of the antenna becomes the height h' above this reflecting plane which is less than the height h above sea level at the antenna.) The calculated curve is subject to slight alteration when the true heights of the experiments become known. The alterations will affect the close range part of the calculated curve, mainly, rather than the long-range part where the earth bulge determines the effect almost entirely. Also shown is a conventional 5/4-earth curve drawn from the value 6 db above free space at the lowest lobe above the horizon to distances well beyond the horizon with the slope of conventional theory, 2.3 $\frac{db}{mi}$. Beyond about 50 miles, the 5/4-earth curve fails utterly to follow the experimental slope of Katzin and Megaw, which is of the order of 0.2 db/mile, very similar to the slope of the internal reflection curve. (A 5/4-earth curve is shown here, because the convenient Booker and Walkinshaw methods use this value rather than 4/3, in order to approximate the refraction due to "dry" atmospheric gases, with no contribution from water vapor.)

c. Additional Experimental Evidence

The third major item of experimental evidence favoring the hypothesis of internal reflection as the explanation of observed distant tropospheric fields comes from the experiments on height gain, or rather the lack of it, as noted by Smyth and the NEL group,[15,16] Katzin and the NRL group,[17] Straiton and the University of Texas group,[18] and others. The observations concerning height gain in [15-18] can be summarized as follows. When the observations are made in the "scatter region", i.e., at distances

and heights such that the diffracted-refracted wave is unobservable, then the observed signal is independent of antenna height, for heights greater than a few feet at K band, or greater than about 100 feet at vhf frequencies. This set of facts receives a very simple explanation in terms of the internal reflection of the lowest lobe of the radiation pattern by the tropospheric stratification. The resultant partial reflection from the normal troposphere is pictured above as being determined by a half-wave layer high over the midpoint of the path, at a height between the lobe maximum and the horizon of the lower of the two antennas. The underside of the lowest lobe is the most important region, because here the glancing angle of the radiation against the tropospheric stratification is as small as possible, subject to condition that the reflections shall occur on a favorable part of the effective vertical antenna patterns, the lobe maxima. Height gain practically ceases above heights which bring the lowest lobe close to the horizon, so that α_T or $\alpha_R \ll \alpha_0$.

The fourth type of evidence strongly supporting the internal reflection hypothesis is the diverse time, geographic, climatic, terrain, and frequency distribution of the accumulated data from high power transmissions. Quantitative data in support of the idea have been mentioned so far coming from vhf data in northeastern U. S., overland 1944-1946; overwater S-band data from the Carribean (1945), the North Sea (1949), the Pacific (1946), and Southern California (1944-); overland microwave data from Arizona desert (1947); overland uhf data from Iowa (1948-1950)[19]. Normal tropospheric stratification here suggested as a cause for the observed nonoptical fields is basically due to gravity itself, which is omnipresent. The earlier suggested explanations in terms of scattering from atmospheric turbulence or earth roughness can scarcely play as widespread a role in the explanation of the data as can reflection from normal tropospheric stratifications.

5. Discussion Of The Integration

The fundamental integration over the whole atmosphere for the internal reflection is that of (2) (when applied to a general stratified medium, this perhaps could be called a Bremmer-type integral[6]). In the foregoing development, an estimate of the integral has been made without direct integration by arguments similar to the famous methods of Fresnel for summing Fresnel zones in diffractional optics, methods generally successful in optics, though admittedly nonrigorous. This choice has been forced for mathematical as well as physical reasons. Mathematically, even if idealized sine function lobe patterns are used for antenna patterns above the horizon, and zero below, the in-

tegral has proved intractable so far to the author.

a. Mathematical Integrations

Feinstein[6,7] has published several results. For a very high antenna, so high that a single lobe covers a height interval small compared to a half-wave layer, he estimates the integral by replacing the sinusoidal fluctuations of a lobe within each half-wave layer by the average value $\frac{2}{\pi}$. The difficulty in utilizing this result lies in the enormous antenna height in wavelengths which would be required to realize its condition experimentally, perhaps microwave frequencies and airplane heights. All the extensive data are groundborne. For "low antennas", Feinstein[7] gives an asymptotic calculation for the case of idealized lobes above the horizon which indicate a small factor $h/\alpha_o D$ in the result for R, where h is an effective antenna height and D the distance, and α_o is the cutoff angle. This result seems to give too small an absolute value for R for explaining average fields at least, and as well to imply a height gain for R in a height region where the data seem clearly to have none. Also it implies no wavelength dependence resulting from the high angle lobes associated with the "low" antenna. The physical meaning of these results is as yet unclear to this author, and may be the subject of a joint communication at a later date. At present, it may be that the smallness of Feinstein's result and (its linear wavelength dependence [6,7]) is a consequence of the idealizations of the model he employs. His antenna pattern functions as used in his (3) may be taken as amounting to replacing the earth bulge by a plane wedge TPR (Fig. 1). Such a model for the earth bulge gives equi-spaced lobes, with perfect nulls, and of course, no reflections from the low-lying atmosphere between P and the earth's surface. If the integration of (1) for the case of a normal static atmosphere with unequally spaced lower lobes, imperfect nulls, and some account of radiation below the horizon, does give a much smaller result than the estimates marked "internal reflection" on Figs. 3 and 4, then the experimental average values will have to be explained in part, at least, by the time variability of the atmospheric index model. Even so, it may not be necessary to invoke the particular type of time variability envisaged by the hypothesis of omnipresent atmospheric turbulence.

It should be pointed out that there is a striking mathematical similarity with the papers of Epstein and Millington in the 1930's, in which the earth bulge was approximated by an opaque knife edge and Huygens' principle was used to estimate the field beyond. For these authors there was no question about internal reflections, but rather of an integration of waves from Huygens' secondary sources from the unobstructed sources above the equivalent knife edge. Millington closed his treatment of the issue (p. 540) on the rather unsatisfactory note that perhaps Kirchoff's

rigorous form of Huygens' principle would not give the $d^{-5/2}$ power law decrease below the horizon, as did Epstein and Millington's application of the simplest form of Huygens' principle. The matter appears to need re-examination.

b. Physical Estimates

In this paper, the difficult integration has been avoided by using elementary optical arguments. The entire atmosphere above the middle of the path is divided into half-wave layers whose thickness $\frac{\lambda}{4\alpha}$ decreases as we go upwards. The half-wave layer of maximum contribution will lie somewhere between the horizon and lowest lobe maximum of the lower antenna. The sign of the contributions from adjacent layers will be alternately + and -. If we add the contributions of the layers not in the sinusoidal order of nature, but rather begin with the largest + zone, then the largest negative, next the second largest positive, then the second largest negative, and so on until all layers have been added, then we have a series of terms of decreasing magnitude and alternating sign $R_1 - R_2 + R_3 - R_4 + R_5 - - - - - -$, to which the famous Fresnel summation arguments may plausibly be implied to infer the estimate $\frac{R_1}{2}$ for the sum.

(See Born's "Optik", pp. 145-146, for a statement of the argument. Note also the sentence before § 46 on p. 151 for the implied limitations on the rigor of the argument.)

A pictorial argument for estimating the integral (2) proceeds as follows. Starting high in the atmosphere, each half-wave layer will contribute half a revolution to a developing spiral in the complex plane as α decreases from $\frac{\pi}{2}$. The spiral will unwind to a maximum radius at each maximum of $f_T f_R$, and shrink to a minimum at each minimum of $f_T f_R$. The largest turn of the spiral will be contributed by what has been called the half-wave layer of maximum contribution below the lobe maximum. The final shrinking of the spiral will be contributed by the weakly illuminated layers below the horizon. The total result will be the closing vector between the beginning of the spiral at great heights and the end of it well below the horizon. For comparison to observed average fields, the average value of the closing vector has been estimated as some not-too-small fraction of the diameter of the largest turn and the value of 1/2 for this function has been used in drawing the curves, from the earlier argument of this section. This amounts to saying that on the average, at least, the total reflected field will be about half that from the half-wave layer of maximum contribution, even in an atmosphere where the index is completely constant in time, and the lobes are all perfectly regular (though not equispaced) as from a perfectly smooth curved earth. (Even

minor and slow time variations in the atmospheric index distribution or commonplace imperfections in the regularity of lobes over a ground surface could reasonably be expected to increase greatly the expected resultant field represented by the closing vector of the spiral. Similarly for any small layers in the atmosphere with a lapse rate of index 4 or more times larger than normal and sufficient to give total internal reflection to energy striking it near grazing. Such deviations from a normal static troposphere are outside the intended scope of this paper.)

To summarize, the agreement of the curves marked "internal reflection" on Figs. 3 and 4 with the points should probably be regarded as the most important basis for the assertion of this paper that a half-wave layer of the normal atmosphere gives internal reflection of the order of magnitude of the average observed fields well beyond the horizon. The arguments justifying these curves as estimates of the resultant internal reflection from the entire troposphere seem plausible physically, and have no adjustable parameters whatever, except for the difficulty of performing the integration over all the normal tropospheric stratification.

c. Further Work

Continued study of both analytical and physically reasonable solutions of the integral (2) over all the layers seems indicated. It must be remembered that the pattern functions f_T and f_R cannot be written down analytically by any known means now, including radiation above and below the horizon. Also, the lobe patterns are never perfectly formed above the horizon, and any analytical treatment should somehow be formulated to see what effect this will cause on the final result if the result is to be used to interpret experimental data. It should also be remembered that, especially at the higher microwave frequencies, the pattern factors f_T and f_R are partially under control of the experimenter who chooses the sizes and vertical tilts of the antennas.

6. The Index Gradient At Large Heights

Because for distances beyond about 200 miles the most important reflection comes from levels above 5,000 feet, it is necessary to take note of the fact that the normal index profile decreases less rapidly at large height than at the surface. (This correction has also been incorporated in Feinstein's published curves[6].) For the normal troposphere, the index of refraction n is well represented as a function of height h by

$$(n-1) = (n_o - 1)\, e^{\frac{-h}{h_s}} \qquad (6)$$

where n_o is the surface value at $h = o$, and h_s is the so-called scale height of the troposphere, in the nomenclature of Fock, who uses the value $h_s = 7.5$ km[22]. Stickland seems to be the first investigator in recent time to note that the form (6) fits the data well over very large ranges of height[23]. Differentiation of (6) gives

$$\left|\frac{dn}{dh}\right| \cong K = K_o\, e^{-h/h_s} . \qquad (7)$$

The values of K corrected to the height of the layer of maximum contribution at the larger distances are the ones to be used beyond a few hundred miles in the formulas of section 3.

7. The Failure Of Conventional Theory

For ten to fifteen years it has been customary to assume that the single mode diffraction theory using an effective 4/3 earth's radius could be accurately corrected for normal tropospheric refraction indefinitely beyond the horizon. It now appears that this is true only out to the point where the 4/3 earth curve falls below the internal reflection estimate, i.e., to about 100 miles on Fig. 3 (50 mc) and 50 miles on Fig. 4 (3,000 mc). The theoretical argument is deducible from Bremmer's paper[8]. He shows that for any plane stratified medium, the Hertz vector π, which is an exact solution of the wave equation for a stratified medium, can be expressed as a series of successive approximations

$$\pi = \pi^{(o)} + \pi^{(1)} + \pi^{(2)} + \pi^{(3)}$$

where $\pi^{(o)}$ is the famous WKB approximate solution, and the other terms $\pi^{(n)}$ represent the contributions of additional waves produced by the stratification and suffering n partial reflections between transmitting and receiving points. The physical meaning of the WKB solution $\pi^{(o)}$ is thus shown to be its complete neglect of all partial reflections. Bremmer's expression for $\pi^{(1)}$, which can be written down from his (23), is, when applied to the troposphere, almost equivalent to Feinstein's expression (2), and may therefore be identified with the internal reflection curves on Figs. 3 and 4. $\pi^{(o)}$, the WKB approximation, may be identified with the 4/3-earth curve. The point where the two curves cross is therefore an indication of the range at which the first order correction equals the value of the zeroth order WKB approximation used to start. As with any successive approximation method, when this happens the zeroth order approximation should no longer be trusted, and a new, more accurate method of solu-

tion looked for. The identification of the 4/3-earth curve with the WKB approximation of Bremmer appears entirely proper, because prior to World War II, at least, the only justification whatever for the use of the effective earth's radius notion well beyond the horizon was the argument given by Eckersley and Millington[24] in 1938, based on their phase integral method, a particular form of the WKB method. (See especially section 8 of [24].)

The agreement with data on Figs. 3 and 4 suggests that we should use the effective earth's radius notion beyond the horizon to give the effect only out to the region where internal reflection in the troposphere becomes dominant; beyond this range, one should use the partial reflections method of Bremmer as first applied by Feinstein. This necessary change from wave to ray methods is already familiar at short ranges within the horizon, where wave modes become increasingly clumsy to compute with, but where simple direct and reflected ray methods are simple and practical. In fact, only once has the wave calculation been pushed very far within the horizon. By summing 17 modes, Van der Pol and Bremmer succeeded in accurately computing by wave methods the field at a range slightly closer than the first lobe maximum. Never has this been repeated, nor need it be. While one will welcome a rigorous quantitative wave solution for the normal troposphere marked "internal refraction", it is hardly likely that such a solution will replace the simple partial ray reflection calculations which fit the data so easily. The mode solution will almost certainly be very complicated, but a few cases should be computed to satisfy our theoretical consciences at least. It is not yet certain why Miller[25] did not find a limitation to the validity of the effective earth's radius notion in his critical reexamination of the rigorous wave theory, but perhaps the use of the same model of the atmospheric index profile as Eckersley and Millington is part of the explanation. This profile misrepresents the index profile at great heights because it approaches a value 0.8 at great heights rather than unity. Discussion of entirely independent work in Russia on the validity of the effective earth's radius notion beyond the horizon by Ponomarew (at Wwedensky's suggestion) and by V. A. Fock will be deferred to another paper.

8. The Bilinear Model For Standard Refraction

The model of the troposphere usually chosen to represent standard refraction in the wave equation is a linear decrease of index of $(12)10^{-6}$ per thousand feet, prolonged indefinitely. Since the surface index starts with a value of (n-1) of $(350 \pm 50)(10)^{-6}$, the linear model cannot possibly make physical

sense above about 30,000 feet at which time the index of the model will have decreased to unity, appropriate to a vacuum. This nonphysical behavior of the linear model at great heights has not hitherto been thought to have importance. The properties of the wave solutions for the bilinear model have been extensively treated by Furry and his collaborators in vol. 13 of the Radiation Laboratory Series (pp. 140-174), in quite another connection, the study of low microwave surface ducts over the ocean. The treatment is quite general enough to be applied to a proposed bilinear model for standard refraction, in which the index is supposed to decrease at the standard rate up to about 30,000 feet, and to remain unity thereafter. The bilinear model seems to possess most of the properties (except ease of calculations) which we should expect to have in a rigorous wave theory of standard refraction which will fit the facts at great distances. Chief among these properties are: (a) It possesses many higher order modes which have lower attenuation than the dominant mode of the linear model; (b) In several numerical examples for microwave surface ducts, it is shown that such slowly attenuating modes can dominate at certain larger distances over the mode of higher attenuation dominant at shorter ranges; (c) As the break in the bilinear curve moves to infinity, the characteristic values of the bilinear model do not go over into the values calculated for a linear model. This seeming peculiarity of the bilinear model, which was once colloquially known as the "skeleton" in the Radiation Laboratory closet, now seems to have important practical significance. Some experimental support has been found for the bilinear model which will be described elsewhere.

9. Implications For Practice

Some rather striking consequences appear to follow from the above notion that high measured tropospheric fields from powerful transmitters at distances of a few hundred miles are perhaps due to weak reflections from the ever-present stratification of the troposphere itself by gravitational forces. Once we admit that the cause of these weak fields is always present, then the possibility must be admitted of reliable communications over these ranges throughout the vhf and microwave spectrum, when sufficiently high power and antenna gains are employed. The chief question which then remains to be answered experimentally is the possibility that other superimposed effects such as duct transmission, elevated layers, scattering from turbulence or insects, or from surface roughness, may so interfere with the weak internally reflected signal as to impair its usefulness by severely limiting the useful bandwidth. None of these obstructive effects seem particularly frequency sensitive, however, and the mere fact that

these weak tropospheric fields fade badly, as do all weak signals, need not make us unduly pessimistic about the practical possibilities. It must be remembered that Megaw has made field measurement out to 360 miles at S band, without superrefraction, using an estimated 30-db more system gain than used by Katzin and the Carribean in 1945 with conventional S-band radar equipment. Note also the very recently published statement by Gerks on p. 1382 of [19].

These rather intriguing possibilities form an interesting comment on how experiment and theory, working together, are a great help to each other, each preventing the other from going astray. Ever since the war, experimental results have been confounding the theory. Now that the theory seems about to catch up with the facts, the understanding of the cause of the discrepancy will probably accelerate sharply the building of higher powered equipment to see what it can do. An historical remark seems pertinent: line-of-sight limitations on the range of radio stations prematurely predicted on the basis of incomplete theory seem to have been a feature of radio history since the very beginning of Marconi's experiments.

10. Conclusion

Although not all the puzzles are yet understood, enough diverse facts and theory have been pieced together to make it appear probable that partial internal reflections in the normal troposphere itself are responsible for the observed slow rate of decrease of field well beyond the horizon of high powered transmitters throughout the vhf and microwave frequency spectrum. This conclusion, when confirmed, has important practical applications. Additional data now available for testing the new theory, additional theoretical developments now foreseeable, and additional crucial experiments should be able to buttress or weaken this conclusion relatively quickly.

11. Acknowledgements

The author wishes to emphasize that the preceding sketch of his present views on the subject represent a crystallization of published ideas which have individually been due originally to a large number of tropospheric propagation researchers active during the last twenty years, although only a few names can be specifically mentioned in such a short outline. A particular intellectual debt is owed to H. Bremmer for his paper on the physical interpretation of the WKB approximation for plane waves passing obliquely through a plane stratified medium, and for his talk on the subject at

a symposium in New York in June, 1950. The author's colleague, Joseph Feinstein, was the first to make a calculation applied to the troposphere of partial reflections, and study of his letter to the editor[6] shortly after it was written (in June, 1951) is gratefully acknowledged. Finally, another colleague, W. Miller, reached a different conclusion from that of this paper, but his paper paved the way for a quicker understanding of the significance of the contributions of Bremmer and Feinstein when they became known after Miller had concluded his work on the subject.

References

1. "Radio progress during 1948. Tropospheric propagation", Proc. I.R.E., vol.37, p.308; March, 1949.

2. "Radio progress during 1949. Tropospheric propagation", Proc. I.R.E., vol. 38, pp. 386-388; April, 1950.

3. "Radio progress during 1950. Tropospheric propagation", Proc. I.R.E., vol. 39, pp. 391-393; April, 1951.

4. H.G. Booker and W.E. Gordon, "A theory of radio scattering in the troposphere", Proc. I.R.E., vol 38, pp. 401-412; April, 1950.

5. Kenneth Bullington, "Propagation of uhf and shf waves beyond the horizon", Proc. I.R.E., vol. 38, pp.1221-1222; October, 1951.

6. J. Feinstein, "Tropospheric propagation beyond the horizon", Jour. Appl. Phys., pp. 1292-1293; October, 1951.

7. J. Feinstein, "The role of partial reflections in tropospheric propagation beyond the horizon", (in this issue of the Transactions).

8. H. Bremmer, "The propagation of electromagnetic waves through a stratified medium and its WKB approximation for oblique incidence", Physica, vol. XV, pp. 594-608; August, 1949.

9. G. Millington, "The reflection coefficient of a linearly graded layer", Marconi Rev. vol. 12, pp. 140-151; October-December, 1949.

10. G. Eckart and T. Kahan, "'Internal' reflection in a stratified medium: particular application to the troposphere", Jour. Phys. Radium, vol. 11, pp. 569-576; October, 1950.

11. A.W. Friend, "Theory and practice of tropospheric sounding by radar", Proc. I.R.E., vol. 37, pp. 116-130; February, 1949.

12. K. Bullington, "Radio propagation variations at vhf and uhf", Proc. I.R.E., vol. 38, pp. 27-32; January, 1950.

12a. E.W. Allen, W.C. Boese, and H. Fine, "Summary of Tropospheric Propagation Measurements and the Development of Empirical VHF Propagation Charts", (revised), FCC report TID 2.4.6; May 26, 1949.

13. E.C.S. Megaw, "The scattering of electromagnetic waves by atmospheric turbulence", Nature, vol. 166, pp. 1100-1104; December 30, 1950.

14. M. Katzin, "Signal Fluctuation in Long Range Overwater Propagation", Report 173, NEL Symposium on Tropospheric Wave Propagation, 25-29, pp. 94-97; July, 1949.

15. L.G. Trolese, "Tropospheric Propagation Characteristics", NEL Symposium, Report No. 173, pp. 17-26.

16. J.P Day and L.G. Trolese, "Propagation of short radio waves over desert terrain", Proc. I.R.E., vol. 38, pp. 165-175; February, 1950.

17. M. Katzin, R.W. Bauchman, and W. Binnian, "3- and 9-cm propagation in low ocean ducts", Proc. I.R.E., vol. 35, pp. 891-905; September, 1947.

18. A.W. Straiton and C.W. Tolbert, "Experimental Discrimination of the Factors in VHF Radio Wave Propagation", University of Texas EERL Report No. 52; 20 June, 1951.

19. Irvin H. Gerks, "Propagation at 412 megacycles from a high-power transmitter", Proc. I.R.E., vol. 39, pp. 1374-1382; November, 1951.

20. G. Millington, "The diffraction of wireless waves around the earth", Phil. Mag., vol. 27, pp. 517-542; May, 1939.

21. P.S. Epstein, "On the bending of electromagnetic microwaves below the horizon", Proc. Nat. Acad. Sci., vol. 21, pp 62-68; 1935.

22. V.A. Fock, "Propagation of the direct wave around the earth with due account for diffraction and refraction", Izvestiya Akademii Nauk, (USSR), vol. XII, no. 2; 1948.

23. A.C. Stickland, "Refraction in the Lower Atmosphere, Meteorological Factors in Radio Wave Propagation", p. 260; 1946.

24. T.L. Eckersley and G. Millington, "Application of the phase integral method to the analysis of the diffraction and refraction of wireless waves round the earth", Phil. Trans. Roy. Soc. Ser. A, vol. 237, pp. 273-309; 1938.

25. W. Miller, "Effective earth's radius for microwave propagation beyond the horizon", Jour. Appl. Phys., vol 22, pp. 52-62; January; 1951.

26. The wavelength and distance dependence quoted in the abstract of the URSI-IRE program held at Ithaca, October 8-10, 1951, results only if the earth reflection is neglected, and the thickness of the half-wave layer above the intersection of the horizons is taken as proportional to $\sqrt{\lambda d}$, as it would be over a plane earth, instead of $\frac{\lambda}{4\alpha_o}$, where α_o is the glancing angle of the cut-off ray at the horizon. The true wavelength and distance dependence is now believed to be much more complicated than mentioned in the abstract, and is believed to be much more plausibly represented by the discussion of section 3 of this paper.

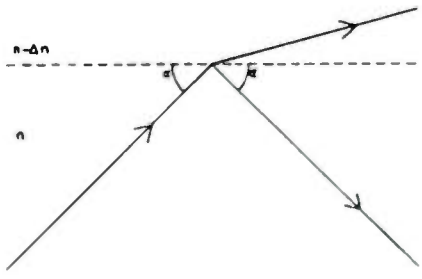

Fig. 1

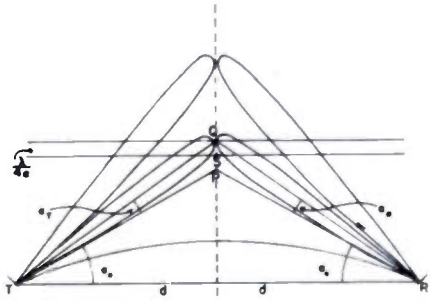

Fig. 2

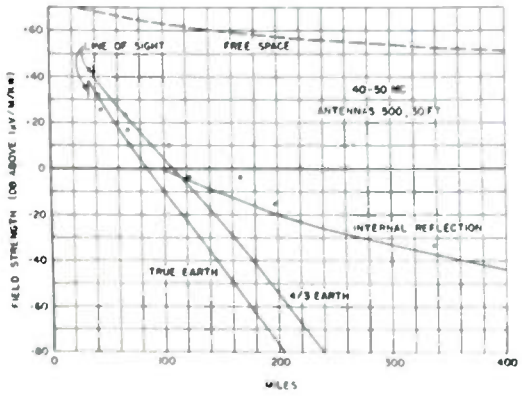

Fig. 3

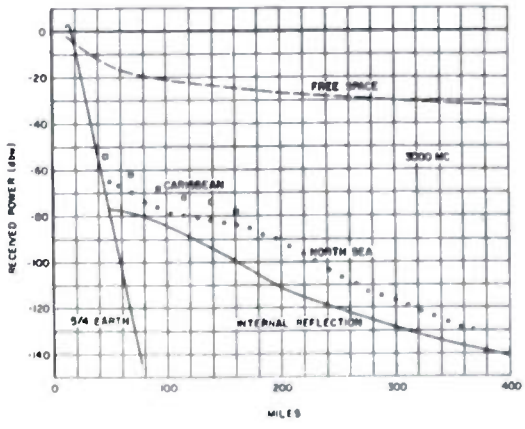

Fig. 4

THE EFFECT OF UNIFORM LAYERS ON THE PROPAGATION OF RADIO WAVES

L.J. Anderson and J.B. Smyth
Navy Electronics Laboratory,
San Diego, Calif.

Introduction

Almost everyone who has studied anomalous propagation in the troposphere will agree that the controlling factors are temperature and humidity profiles along the propagation path. However, when one tries to correlate propagation data against refractive index profiles as computed from temperature and humidity data, one immediately encounters the difficulty of a large scatter of points. In this case, one is often tempted to attribute the scatter to unknown influences which have not been taken into account.

In the opinion of the authors and many others, much of the difficulty lies in the fact that uniform horizontal stratification is rarely achieved. Since stratification is one of the first assumptions made in any theoretical approach to the problem, it is apparent that nonuniformity may render the theory inapplicable to most field data. It therefore seems essential, when attempting to compare observed data with theory, to eliminate all data for which horizontal uniformity cannot be proven.

The data presented in this paper have been selected with this requirement in mind, and although the data are not too numerous, it seems that their selection has resulted in materially improved correlation and agreement with theory.

The data were obtained on a 90-mile propagation link along the coast of Southern California. The transmitter and receiver heights were both 100 feet, and propagation was entirely over water. Fig. 1 shows the general location of the path with respect to the coast line. The meteorological situation for this area has been adequately described elsewhere[1] and consists of a layer of cool, moist marine air of varying thickness overlaid by a warm, dry layer. This results in an elevated inversion the height of which varies from day to day over a range from the surface to 5,000 feet.

The propagation data presented consist of field strength observations selected from continuous recordings made at 52, 100, and 550 mc. The meteorological soundings were taken by means of an airplane which made a number of ascents and descents as it flew along the path. Generally, about six such soundings were made within the space of an hour. A total of 47 days of such data were obtained. After eliminating all days in which the individual soundings did not show essentially uniform stratification, a total of eight days was left.

Fig. 2 shows the soundings taken for each of these days. All soundings taken on a given day are superimposed to show the degree of uniformity existing.

To illustrate the scatter obtained when uniformity conditions are not observed, two sets of propagation data are plotted against single-sounding meteorological data. In the first set, the meteorological data were obtained at a point near the south end of the propagation path by means of wired sonde equipment. In the second set, meteorological data were obtained by a wired sonde located at the middle of the path. Field strength observations in both of these cases were taken in the same way as outlined above.

Correlation of Field Strength with Layer Height

Fig. 3 is a plot of the height of the top of the inversion layer as measured by the La Jolla wired sonde against the maximum field strength at 550 mc observed during the hour when the sounding was made. The scatter of points in this case is fairly large. The correlation coefficient is 0.57, which is barely significant. A definite trend is discernible with higher field strengths occurring with lower layers, but little else can be deduced from the data.

Fig. 4 is a similar plot using the wired sonde at the middle of the path. In this case, the correlation coefficient is 0.78 which is somewhat better than that in Fig. 3, but still not very satisfying. Since one would expect the least effect of nonuniformity when soundings are taken at the midpoint of the path, it is apparent that this is about as good a correlation as we can attain using a single-sounding data.

In both of these cases only those data were used in which the refractive index change through the layer was between 30 and 50 units. This selection eliminated some of the scatter due to varying inversion strength.

Figs. 5, 6, and 7 show similar plots at 52, 100, and 550 mc, respectively, in which the meteorological data were obtained by airplane soundings, and only those days showing uniform stratification have been plotted. The observed data are plotted on solid dots, It is immediately apparent that the correlation in these figures is much better than that obtained with single-sounding data. Although only eight points were available, the shapes of the curves are readily apparent.

Calculated Fields

1. Reflection from Smooth Layers

In Figs. 5,6, and 7, the field strengths calculated on the basis of a single reflection from the layer at the midpoint of the path are shown as open circles. The reflection coefficient for smooth layers may be obtained from the relation:

$$R = \frac{\sinh^2 p\pi(\sin\alpha - \sqrt{\sin^2\alpha - \sin^2\beta}}{\sinh^2 p\pi(\sin\alpha + \sqrt{\sin^2 - \sin^2}}$$

where: $\Delta p = 1.07 \frac{\Delta h}{\lambda}$ and $\sin^2\beta = 2\Delta B$

α is the grazing angle of incidence of the wave on the layer,

Δh is the thickness of the reflecting layer, and

ΔB is the change of refractive index through the layer.

For layer heights below 500 feet, the midpoint lies below the horizon, hence it is necessary to use a multi-hop mechanism. In this case, reflection from the layer was considered to occur at the critical angle. The fields were calculated using height-gain values at the point of reflection and assuming unity reflection coefficient. The multi-hop calculations are plotted as open triangles on Figs. 5,6, and 7. It will be observed that the assumption of a smooth layer yields good agreement with the fields observed on 52 mc. The agreement is almost as good at 100 mc. At 500 mc, however, the smooth layer fields depart radically from observation for

layer heights above 1,700 feet.

2. Reflection from Sinusoidal Layers

It has often been observed, when flying above the cloud deck which forms the base of the elevated inversion layer, that the layer exhibits Helmholtz waves as would be expected from the difference in density between the two air strata[1]. The amplitudes of these waves appear to be of the order of 100 feet, and the wavelengths vary from a few thousand feet to several miles. The presence of such waves would cause the reflecting stratum to depart radically from the smooth case considered above, for wavelengths small compared to the amplitude of the undulations. Rigorous mathematical treatment of the reflection of electromagnetic energy from sinusoidal surfaces is extremely complex, if not impossible. However, certain approximations can be made which greatly simplify the problem. In Fig. 8, consider a portion of the stratum as shown by the curved line and a plane wave incident at an angle α with horizontal. If one considers that an appreciable amount of energy will be reflected only from the portion of the surface which makes an angle with the incident radiation less than that required for total reflection, then one can solve for the fraction of the total sinusoidal surface from which reflection occurs.

Admittedly, this concept is approximate, but since the reflection coefficient falls off very rapidly for angles greater than β, the approximation would seem to be reasonably good. For computing the fraction of the total surface from which such reflection occurs, we use the following:

Assume the layer shape is $z = a \sin bx$

$$\frac{dz}{dx} = ab \cos bx = \theta \qquad \text{for small angles}$$

then $x_1 = \frac{1}{b} \cos^{-1} \left(\frac{\alpha-\beta}{ab}\right)$ where $\beta = \sqrt{2\Delta\beta} \times 10^{-3}$

$x_2 = \frac{1}{b} \cos^{-1} \left(\frac{\alpha}{ab}\right)$ and $L = \frac{2\pi}{b}$

thus: $\frac{x_2-x_1}{L} = \frac{1}{2\pi} \left(\cos^{-1} \frac{\alpha}{ab} - \cos^{-1} \frac{\alpha-\beta}{ab}\right)$.

Since most of the energy will be reflected from these elements at angles other than α, it is also necessary to take into account the diffraction pattern of the individual elements. This is accomplished by using the familiar relationship

$$\frac{I}{I_o} \quad \frac{\sin^2 \gamma}{\gamma^2}$$

where $$\gamma = \frac{2\pi(x_2 - x_1)}{\lambda} \sin \alpha \sin \theta .$$

To calculate the maximum intensity of the main lobe of the diffraction pattern, we use

$$\frac{I_{max}}{I_o} = \frac{(x_2 - x_1)^2 \sin \alpha}{\lambda \, D}$$

where D is half the propagation path length.

This gives us the fraction of the total incident energy which is reflected at an angle α, which is the optimum for reception.

The method of calculating the energy reflected from such a sinusoidal surface will then be to compute the height-gain at the midpoint of the path for various layer heights over the range of 500 to 3,000 feet, and to reduce these values by the fraction of energy reflected from the sinusoidal elements as calculated above. Since the received energy is a summation of the energy reflected from a number of such elements, the reflected wave is no longer a coherent wave front, and hence we assume that these individual wavelets arrive at the receiver with random pause.

In Figs. 5, 6, and 7, the points marked with X's denote the field strengths computed in this manner. It will be observed that these values lie below the smooth layer calculations except in the case of the highest frequency (550 mc).

At this frequency it appears that the layer is becoming rough. For these calculations, the best agreement with observation is found using the shape factor $a/L = 0.004$ where 2a is the total amplitude and L is the wavelength of the undulation. For example, if 2a is 100 feet, L will be approximately 2½ miles, which is of the order of magnitude of observed undulations.

Reference

1. J.B. Smyth, L.G. Trolese, Proc. I.R.E., vol. 33, pp. 1198-1202; November, 1947.

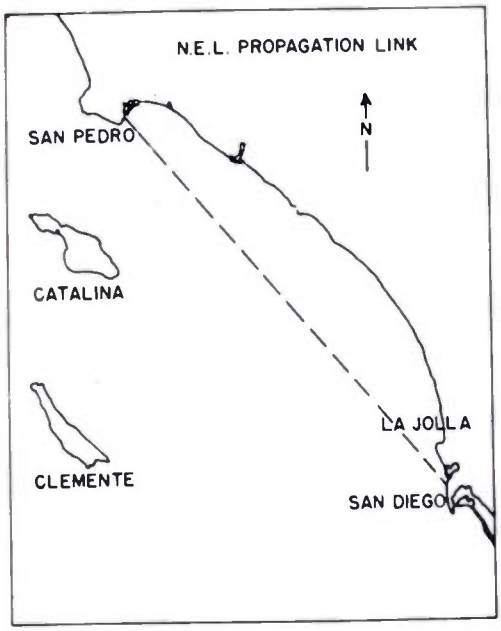

Fig. 1

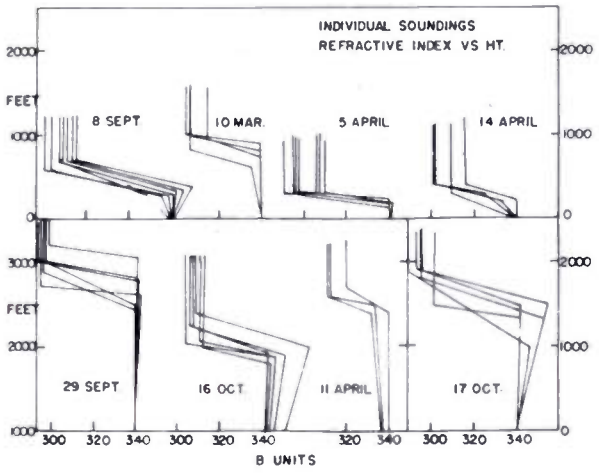

Fig. 2

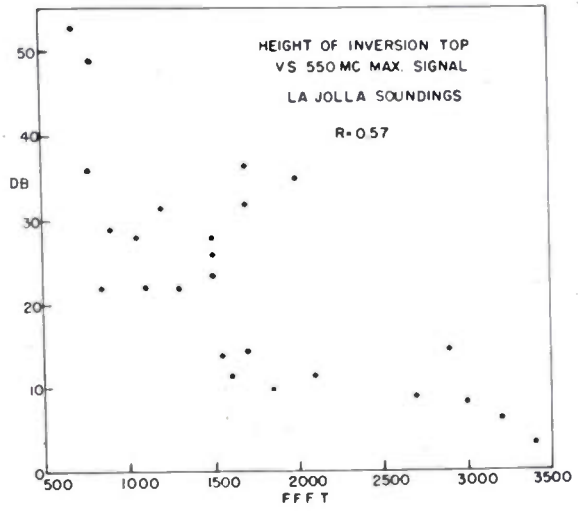

Fig. 3

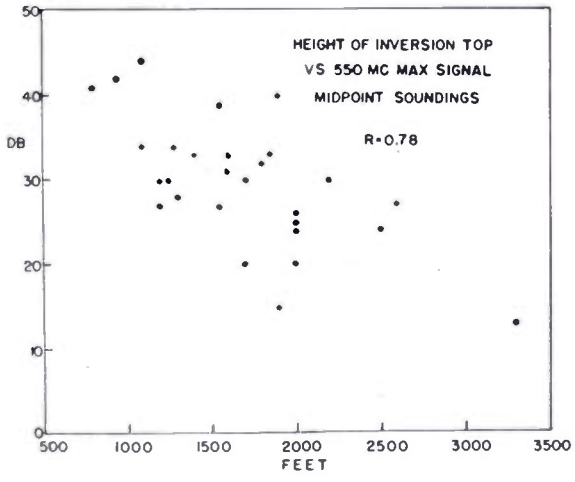

Fig. 4

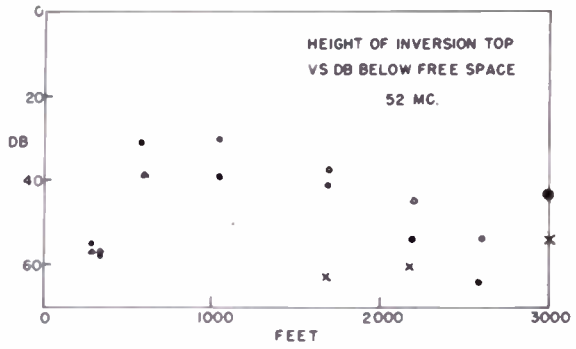

Fig. 5

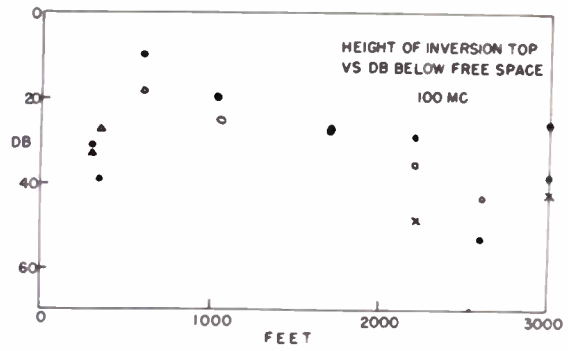

Fig. 6

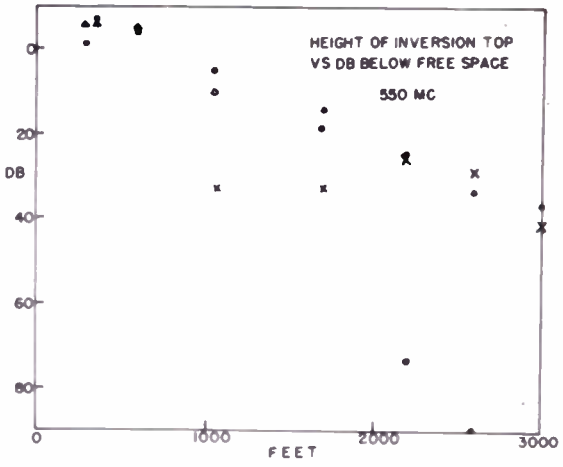

Fig. 7

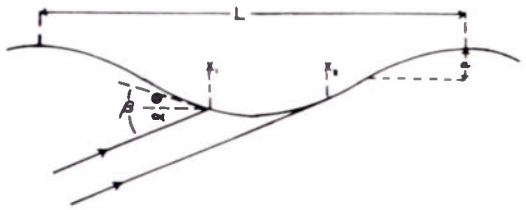

Fig. 8

FIELD STRENGTHS RECORDED ON ADJACENT FM CHANNELS AT 93 MC OVER DISTANCES FROM 40 TO 150 MILES

G.S. Wickizer and A.M. Braaten
RCA Laboratories Division,
Riverhead, L.I., N.Y.

Field strengths of KE2XCC (93.1 mc, Alpine, N.J.) and WBZ-FM (92.9 mc, Boston, Mass.) have been recorded for more than a year at two locations (Hauppauge and Riverhead) on Long Island. The distances from Alpine to the receivers were 40.5 and 67.2 miles, while from Boston they were 150.4 and 127.4 miles. Statistical analysis of data for the evening hours reveals a broad seasonal trend toward higher intensities in the summer, with larger over-all variation on the longer transmission paths. Based on analysis of one summer month, refraction effects appeared to vary independently in the two directions. The ratio of field strength between the near and distant transmitters, analyzed with respect to time, was found to approach a normal probability distribution at Riverhead, and a Rayleigh distribution at Hauppauge. During periods of violent fading, hourly median field strengths of WBZ-FM varied over a range of 23 db at Riverhead and 19 db at Hauppauge. For the same periods, the ratio between Riverhead and Hauppauge fields varied over a considerable range and occasionally became less than unity.

(Abstract)

REFRACTION OF RADIO WAVES IN ARBITRARY ATMOSPHERE-RAY-TRACING PICTURE

Ming S. Wong
Wright-Patterson Air Force Base,
Dayton, Ohio

A development following Hartree, etc., is carried out of ray tracing using REAC differential analyzer. Ray families, on 24-inch by 32-inch paper, are obtained for an atmosphere with a single n profile (index of refraction versus altitude curve), and for an atmosphere with three n profiles over the region of interest. The n profiles used were measured up to 10,000-foot altitude.

The variation in radio field strength with separation between airplanes as measured in a recent air-to-air propagation flight is correlated with a variation of ray density based on index of refraction data taken during the flight. This was a flight which encountered a radio hole followed by its anti-hole (region of enhanced and interfering signals) within the geometrical horizon, and then a second hole and anti-hole at an anomalously large range beyond the horizon. The second anti-hole is accounted for by an anomalous-range layer near the ground and one in which the refractive gradient has a negative value nearly equal to 1/(radius of earth).

In some respects the correlation is striking between ray-tracing picture and observed radio data.

(Abstract)

SOME CHARACTERISTICS OF TROPOSPHERIC SCATTERING*

A. H. LaGrone
University of Texas
Austin, Texas

Three problems are considered in this paper which are important in determining the effect of scattering on distant radio fields.

The first problem is the attenuation of radio signals caused by scattering[1]. Booker and Gordon[2] supposed secondary scattering to be negligible, and proceeded to develop the general equation for scattering without including this component. This paper shows their assumption to be valid by determining the total power scattered per unit macroscopic element of volume relative to the power incident on the volume.

The second problem is a volume integration to determine the total scattered signal reaching a receiver point[3]. An equation is developed in terms of the propagation parameters which will give this total signal.

The third problem is that of cross polarization[4] in the scattered wave. In working on the second problem, it was noted that a difference in polarization existed in the scattered signal which came from different elements of the scattering volume. A system of dipoles at right angles to each other was then assumed, and equations developed for determining the scattered signal received on each of these dipoles. Numerical examples were computed and are compared with field measurements of the cross polarized signal.

(Abstract)

References

1. A.H. LaGrone, W.H. Benson, Jr., and A.W. Straiton, "Attenuation of radio signals caused by scattering", Jour. Appl.

* This work was sponsored by the Office of Naval Research under contract N5ori-136, P. O. I.

Phys., vol. 22, pp. 672-674; May, 1951.

2. H.G. Booker and W.E. Gordon, "A theory of radio scattering in the troposphere", Proc. I.R.E., vol. 38, pp. 401-412; April, 1950.

3. A.H. LaGrone, "Volume integration of scattered radio waves", (to be published in Proc. I.R.E.).

4. A.H. LaGrone, "Cross polarization of scattered radio waves", Elec. Eng. Res. Lab., The University of Texas, Report No. 48, 1951.

THE DIELECTRIC PROPERTIES OF ICE AND SNOW AT 3.2 CENTIMETRES AS RELATED TO THE REFLECTION COEFFICIENT OF SNOW-COVERED SURFACES

W.A. Cumming
National Research Council
Ottawa, Canada

A study has been made of the reflecting properties of snow- and ice-covered surfaces at a wavelength of 3.2 centimeters. In making this study, two lines of investigation have been followed. In one, controlled laboratory measurements were made of the permittivity and loss tangent of ice and snow of varying density and crystal structure over the temperature range 0° to -20° C, using waveguide techniques. In the other investigation, direct measurements were made, on an outdoor range, of the reflection coefficients of a flat metallic surface covered with snow.

As a result of the measurements using waveguide techniques, curves have been obtained of snow permittivity as a function of density; and of snow and ice loss tangent as functions of temperature, density, and crystalline structure. To a first approximation, the permittivity epsilon of snow of density rho is given by epsilon equals epsilon zero e to the rho over rho zero power; where epsilon zero and rho zero are the dielectric constant and density of ice, and epsilon is independent of temperature in the range 0° to -20° C. The permittivity of ice was found to be 3.15.

The loss tangent of ice was found to vary considerably with temperature, having a value of 27×10^{-4} at 0° C, and a value of 6×10^{-4} at -20 ° C. The loss tangent of snow, on the other hand, was found to vary over wider limits, being a function not only of density and temperature, but also of crystalline structure.

When these results are applied to the study of reflection coefficient, two facts are evident: the magnitude of the first reflection at an air-snow boundary is greater than was thought previously, and the attenuation through snow is also greater.

These conclusions are borne out qualitatively by the results obtained on the outdoor range. The measured reflection coefficients were found to be dependent to a considerable extent on snow temperature, and the effects of multiple reflections were not as great as had been anticipated. Several interesting curves of reflection coefficient versus grazing angle have been obtained for flat metal surfaces covered with snow.

(Abstract)

RADIO WAVE PROPAGATION OVER LONG DISTANCES AT 100 KC

Capt. Oscar Goldberg
Rome Air Development Center
Griffiss Air Force Base,
Rome, N. Y.

and

Dr. Richard H. Woodward
Pickard and Burns, Inc.
Needham, Mass.

With the assignment of the 90- to 100-kc band to long-distance navigation systems, the interest in obtaining fairly precise propagation information for these frequencies has rapidly increased. Because of the lack of a suitable method of computing the level of received composite signal at various distances from a transmitter, it was decided to obtain this information experimentally.

This work will be done in two phases. The first phase, using a continuous wave transmitter at 100 kc, has been completed and will be reported here. The purpose of this portion of the work was to determine when one could receive a signal which would be useful above the normal atmospheric interference. The second phase, which will employ the transmission of "short" pulses, will enable one to separate the various modes of the received signal, and so determine its composite characteristics more precisely.

Since the beginning of July, 1950, a transmitting station at Allaire, New Jersey, latitude 40° 10' 30" N and longitude 74° 8' 36" W, has been radiating continuous-wave signals at 100 kc from a 300-foot antenna. Transmissions were on once a week between 8 o'clock (1300 GCT) Tuesday morning and 8 o'clock Wednesday morning. The radiated power was approximately 800 watts. The transmitter sequence consists of an "on" period for ten minutes and "off" period of five minutes during which time the noise field intensity was measured at the monitor stations. The transmitter was placed in operation and reliable and routine monitoring commenced in September, 1950. Recordings were made until the end of July, 1951.

As a check on the proper functioning of the transmitter, the radiated signals were received and recorded at short ranges, first at Red Bank, New Jersey, and later at Adamston, New Jersey. These and other short-range measurements made with Model AN/URM-6 field intensity meters gave field intensities corresponding to 150 mv per meter at one mile from the transmitter. Variations from this value were applied as corrections to the received signal levels.

The monitor receiving stations were located at universities in North Carolina, Indiana, Iowa, Nebraska, Colorado, and California. These sites are shown on Fig. 1. This map is a copy of the FCC map of the United States showing ground conductivities. The signal and noise field intensities were recorded continuously on Esterline-Angus recorders for a 24-hour period every week. The monitor station receiving equipment consisted of a 59-foot Lingo mast antenna connected through a suitable coupling unit to a modified National Model HRO receiver. A bandwidth of 1.2 kc at 6 db down and 10.4 kc at 60 db down was used. The IF signal was introduced into a special detector, filter, and cathode follower circuit, which operated the Esterline-Angus recorder. These circuits had an integrating time-constant of about 5 seconds and an output that was logarithimatically related to the receiver input. The receiving equipment was periodically calibrated with reference to standard signals from a Model 605-C signal generator. The antenna constant for the mast at each installation was determined by comparing the measured voltage induced at the receiver input by the AN/URM-6 field intensity meter. Because of the poor signal-to-noise ratios at Stanford, a receiver having a bandwidth of 5 cps and a special loop antenna were used for measuring field intensities.

A sample record showing the signal sequence as received is shown in Fig. 2. This tape shows the variation of signal and noise as a function of time.

In general, sky-wave field intensities vary with the time of day, season, and latitude of the point of reflection in the ionosphere; they also vary with the sun-spot cycle, geomagnetic activity, and sudden ionospheric disturbances which are associated with solar activity. Since the characteristics of sky-wave propagation are determined by the distribution of ionization density in the upper atmosphere, which in turn depends upon solar ultraviolet radiation, it was convenient to consider sky-wave propagation in terms of the intensity of ultraviolet radiation. This is related to the cosine of the sun's zenith distance X. In this way, three in-

dependent variables, time of day, season, and latitude, may be replaced by a single independent variable, cos X, as shown by the equation

$$\cos X = \sin \delta \sin \varphi + \cos \delta \cos \varphi \cos t \qquad (1)$$

where δ is the sun's declination, φ is the latitude of the point of reflection, and t is the hour angle at the point of reflection.

Although the processes by which the ionization is produced and sustained, especially at night, are not well understood, and the concept of the ionization varying with cos X at night has no physical significance, it has been found experimentally that the observed field intensities, and presumably the ionization densities, do vary in a regular fashion with cos X. Because it was convenient, and previous experience with the Low Frequency Loran observations has demonstrated its usefulness, the analysis with reference to cos X has been adopted for the ground monitor data in this study of radio propagation at 100 kc.

In analyzing the data (see Fig. 2) the recorded voltages have been averaged visually over 5-minute periods, scaled off on a logarithmic scale, which is referred to voltage calibration markers, and tabulated. The resulting measured voltages have been multiplied by the antenna constant for the particular monitor station to give the measured field intensity in mv per meter. The noise intensity is measured during the 5-minute period between transmissions. For each of the two 5-minute periods before and after the noise measurement, the measured signal-plus-noise intensity is corrected for the noise contamination on the assumption that the observed intensity is equal to the square root of the sum of the squares of the noise and signal intensities. Root-mean-square averages of the noise and signal intensities have been calculated for half-hour periods. The records from the short-range monitors at Watson Laboratories, and later at Adamston, have served as checks on the proper operation of the transmitter.

Some 40 plots showing the half-hourly averages of the received signal intensities as observed at the 6 monitor stations have been plotted. Fig. 3 is one example. In order to condense the information, the half-hourly averages have also been tabulated with respect to cos X. The root-mean-square averages for fall, winter, and spring have been plotted against cost X. Figs. 4 through 13 show this information. The results of the analysis of the ground monitor data are

are expressed as root-mean-square averages. The amount by which any single observation differs from this average cannot be predicted, but it can be estimated from the probable error. If the distribution of the deviation follows the gaussian normal law, as it does within acceptable limits, then there are as many deviations that are greater than the probable error as there are deviations that are smaller. The standard deviation is shown by length of the straight line through the circle which shows the average value.

One interesting factor is the symmetrical nature of the curves about the axis of cos X = 1 (when the sun is at its zenith). The field intensities increase in the morning and afternoon as cos X approaches zero (when the sun is on the horizon). In the evening, as the sun sinks below the horizon with negative values of cos X, the ionization density in the absorbing regions decreases and the observed field intensities increase. In the early morning, as the sun approaches the horizon, the field intensities decrease with decreasing negative values of cos X. The fact that in general the curves for negative as well as positive values of cos X are symmetrical with respect to the axis of cos X = 1 indicates that the conventional concept of an ionization density that steadily decreases throughout the night fails to give a true picture of the ionosphere as it is reflected by low frequency signals. The similarity of the curves for different seasons indicates that the variation through the seasons is due primarily to the variation of solar ultraviolet light intensity, and that the field intensity at any time of day or season can be predicted with satisfactory reliability from a knowledge of cos X and of the general variation of field intensity with cos X.

The data from the ground monitor stations yielded first the average daytime and nighttime field intensities received. Since most of the early work on low frequency propagation has been expressed in terms of the Austin-Cohen formula, it seemed appropriate, first, to compare the observed averages with the field intensities derived from that equation.

If the appropriate value of τ and the measured field intensity of 150 mv per meter at one nautical mile are substituted in this equation it becomes

$$\mathcal{E} = \frac{277}{d} \sqrt{\frac{\theta}{\sin \theta}} \; e^{-0.00087d} \qquad (2)$$

and yields the field intensities for the 6 monitor stations.

The agreement with the observed daytime intensities was only fair, since the Austin-Cohen formula was derived from daytime observations over seawater at very low frequencies (most of them below 100 kc). The equation obviously gives no information concerning diurnal and seasonal variations or the effect of ground constants.

The nighttime signal will be predominantly affected by the sky-wave signal. The intensity of the sky-wave signal depends on the intensity E_0 at unit distance, the length d_s of the sky-wave propagation path, the antenna gains, and the ionospheric and ground reflection coefficients R_s and R_g. For vertical transmitting and receiving antennas, the following equation expresses the intensity of an n^{th}-hop sky-wave signal with reasonable accuracy:

$$\mathcal{E}_{sw} = \frac{E_0}{dn} \cos^2\varphi \, R_s^n \, R_g^{n-1} \qquad (3)$$

where φ is the angle of take-off, R_s is the ratio of the intensity of the wave reflected from the ionosphere to the intensity of the incident wave, and R_g is the corresponding ratio for the wave reflected from the ground. The ionospheric reflection coefficient can best be related to the cosine of the sun's zenith distance at the point of reflection and on the frequency. Observations at 100 kc indicate that the average ionospheric reflection coefficient is 0.15 during the day and 0.6 at night. The actual variation of the reflection coefficient with the cosine of the sun's zenith distance is shown in Fig. 14. The theory of reflection at the ground is well developed and the value of the ground reflection coefficient can be readily determined if the ground constants are known. Examples of ground-wave, sky-wave, and composite field intensities computed for typical day and night conditions are compared with the averages observed at the monitor stations and are shown in Figs. 15 and 16. The circles are average data for the individual monitor stations.

The observed sky-wave field intensities and the ionospheric reflection coefficients at 100 kc depend upon the height at which reflection takes place and on the gradient of the density of ionization at and below that height. The distribution of ionization in the upper atmosphere depends in a complicated fashion on the intensity of ultraviolet radiation which is associated with solar activity and solar flares; it may also depend upon geomagnetic and ionospheric activity. In an effort to find the variation of the average field in-

tensity with these quantities, the average daytime and nighttime field intensities for each weekly period of observation and for each of the 6 monitor stations have been plotted against the days of the year. The I character figures of ionospheric storminess as observed at Washington, D.C. and the geomagnetic K character figures as observed at Cheltenham, Maryland, are also to be shown for these same periods (Figs. 17 and 18). Although in one case the peak of geomagnetic and ionospheric activity is accompanied by a dip in the nighttime field intensities, no consistent change is associated with other peaks of activity. Furthermore, there seems to be no tendency for the intensities as measured at the different monitor stations to rise and fall together, as they might be expected to do if the density of the ionization over a large area increased or decreased, or if the reflecting layer rose or fell under the influence of ultraviolet radiation or geomagnetic activity. The failure of the average day and night field intensities, as observed at the different monitor stations, to vary consistently and systematically, indicates that over periods of a few hours the field intensity at any station is controlled less by the ionosphere reflection coefficient than by the random effects that result from a rough ionosphere. Apparently the interference patterns vary slowly and therefore do not cancel out over the day or night.

In addition to the ground monitoring, flight tests were made to obtain supplementary data which would serve to link the ground data together. A total of thirteen flight tests performed entirely either during the day or night were made. These round trip flights were to distances of 2,200 n. miles. Most of the flights were made in a C-54 aircraft with an insulated tail fin which served as an antenna. The antenna was connected through a coupling unit and coaxial cable to one of two field intensity meters. Early test measurements were made manually with a Model TS-635/UP field intensity meter. Later tests also used the Stoddard AN/URM-6 field intensity meters with Esterline-Angus recorders. These field intensity meters normally have a bandwidth of 400 cps., but for recording signals at great distances the bandwidth of one of them was reduced to 15 cps by the addition of a crystal filter. On most of the flights the field intensities were recorded simultaneously by two field intensity meters. The calibrations of the field intensity meters were checked periodically by calibration signals, and the antenna constants were measured on the ground before each flight. The agreement between the curves obtained with individual meters demonstrates the reliable performance of the equipment. Received field strength variations as a function of distance, terrain,

and season were obtained (Figs. 19 and 20). Flights were also made over water.

The effect of noise was shown as a function of cos X also. Figs. 21 and 22 plot the signal-to-noise ratios observed for the various distances as a function of cos X.

Only representative samples have been presented here. The complete data are available in a report published for the U.S. Air Force by Pickard and Burns, Inc. entitled "The Evaluation and Analysis of 100 kc Radiation Data". Copies of these reports are available from the Rome Air Development Center, Griffiss Air Force Base, Rome, N.Y.

The second phase of this 100-kc propagation program is aimed at learning the composition of the received signals at long distances. This will be attempted by the transmission of pulses short enough to provide mode separation. It is planned to transmit pulses of not more than 50 microseconds in length. A 1-megawatt, 100 kc pulse transmitter feeding a 1,200-foot vertical mast are being modified for this purpose. It is proving rather difficult, nevertheless, to radiate this "short" pulse with any appreciable power. At the receiving sites as yet undecided upon, it is planned to record the amplitude, phase, time-delay, and polarization of the individual modes.

Acknowledgements

The Authors are indebted to Drs. L.P. Wheeler and G.W. Pickard of Pickard and Burns, Inc. for their invaluable assistance in the data reduction and analysis; to Mr. J.A. Pierce of Cruft Laboratories, Harvard University, and to Mr. H.P. Blanchard of Stanford University for their guidance in planning and accomplishing this task. In addition, our appreciation is extended to the faculties and student bodies of North Carolina State College, Rose Polytechnic Institute, Parsons College, Hastings College, University of Colorado, and Stanford University for their assistance in the data collection.

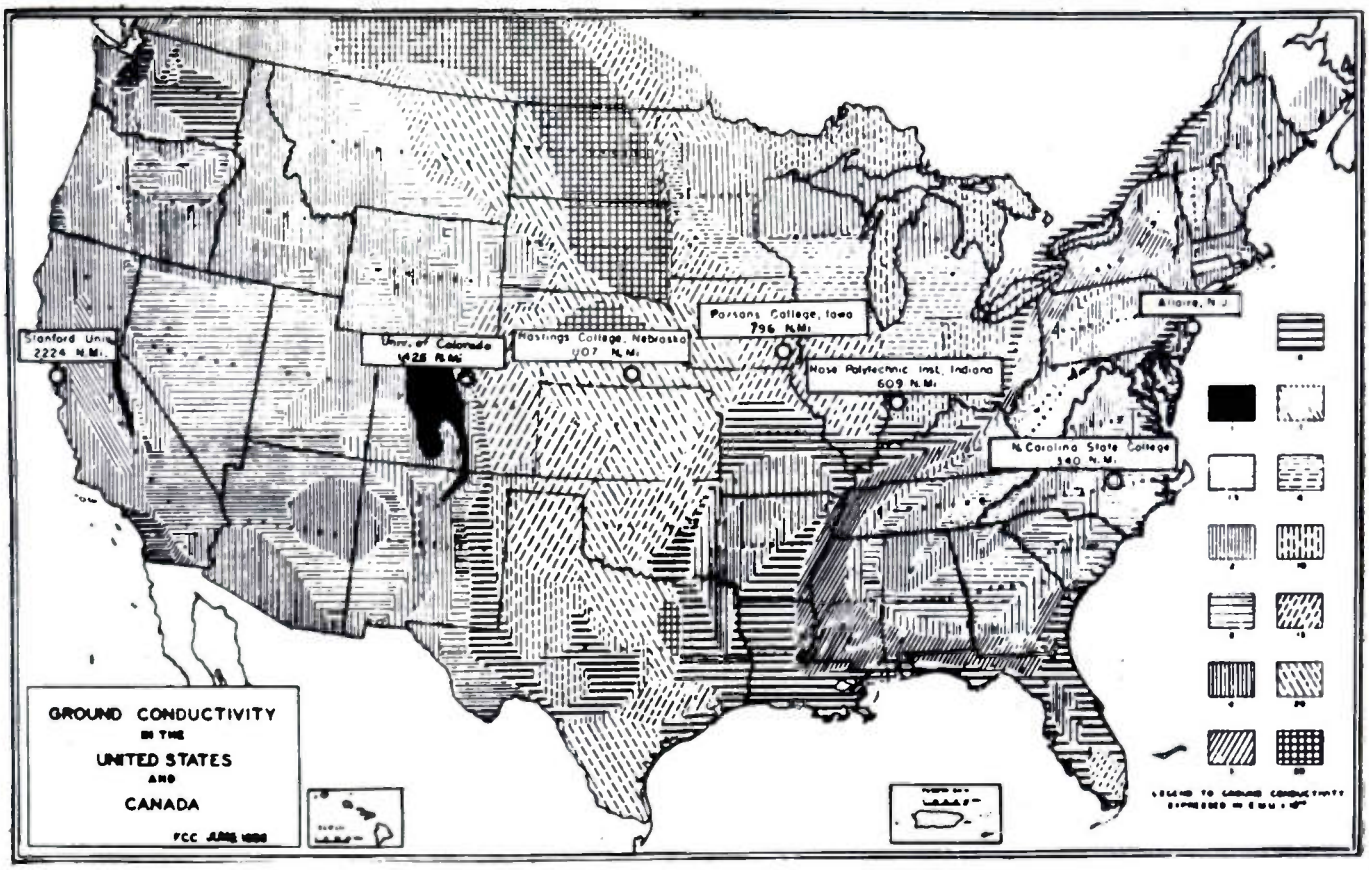

Fig. 1

Map of United States showing ground conductivities and location of ground monitor stations

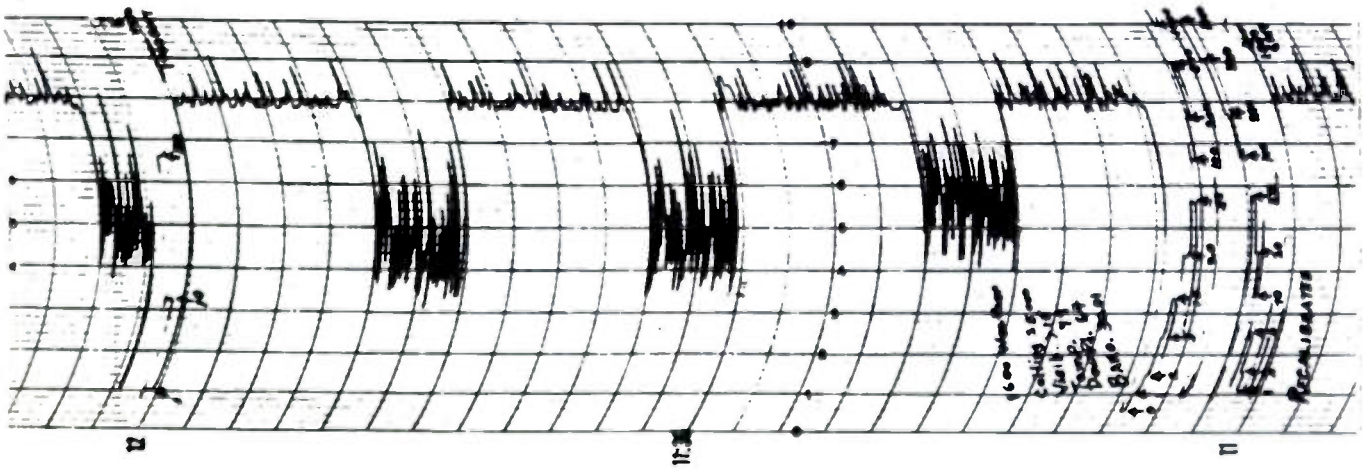

Fig. 2

Specimen of record tape

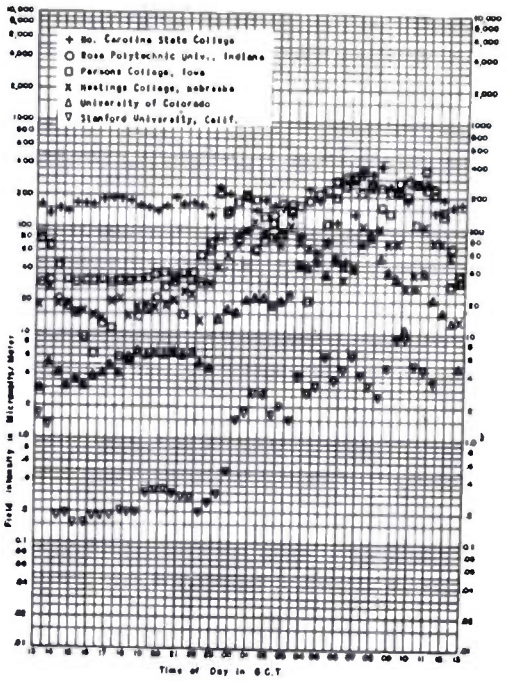

Fig. 3

Summary of field intensity measurements, December 12-13, 1950

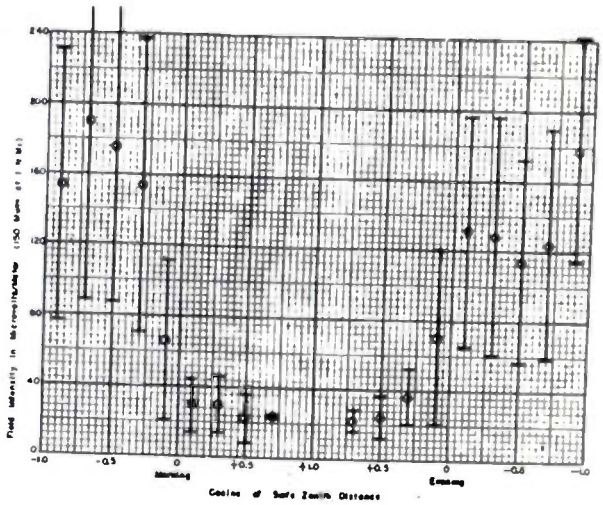

Fig. 4

Variation of winter field intensity with cosine of sun's zenith distance at Rose Polytechnic Institute (609 N. miles)

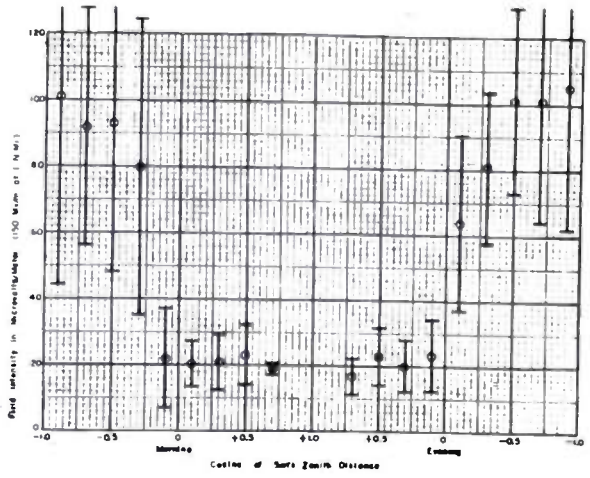

Fig. 5

Variation of winter field intensity with cosine of sun's zenith distance at Hastings College (1,107 N. miles)

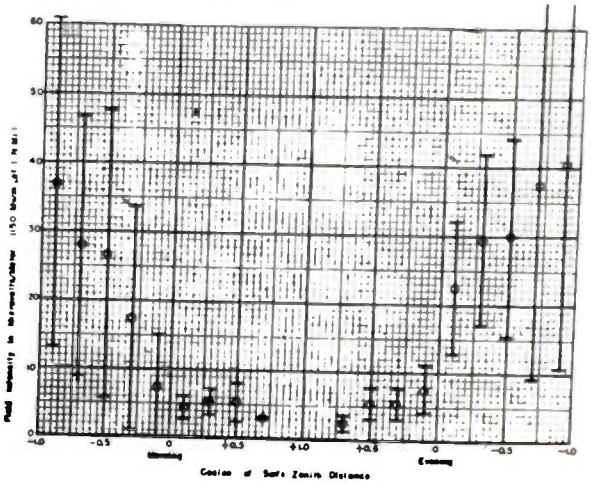

Fig. 6

Variation of winter field intensity with cosine of sun's zenith distance at University of Colorado (1,424 N. miles)

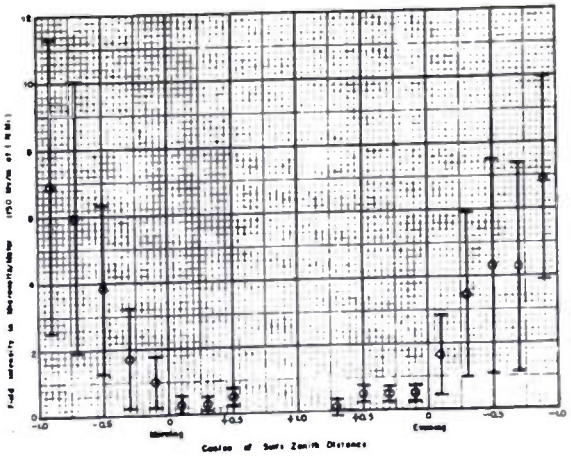

Fig. 7
Variation of winter field intensity with cosine of sun's zenith distance at Stanford University (2,224 N. miles)

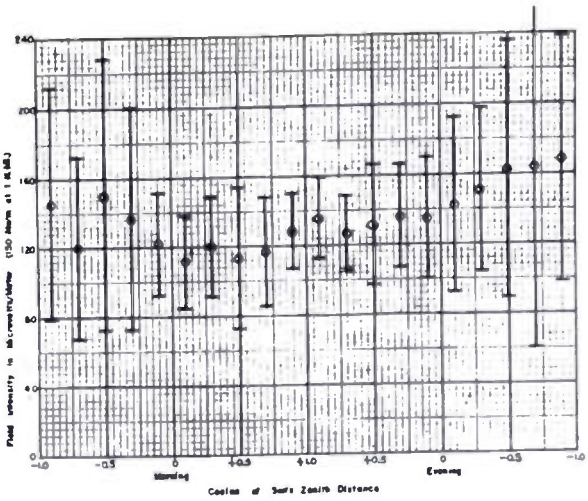

Fig. 8
Variation of spring and fall field intensity with cosine of sun's zenith distance at North Carolina State College (340 N. miles)

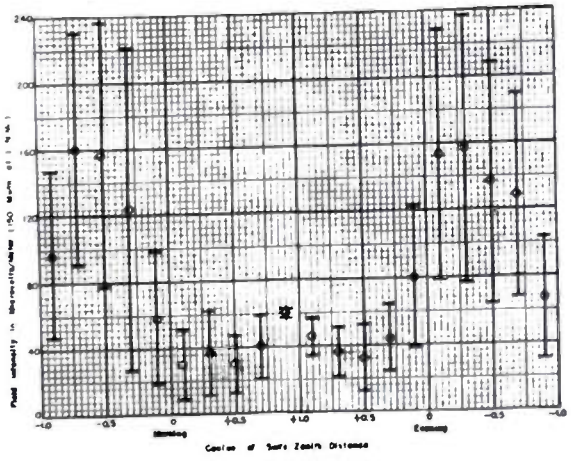

Fig. 9
Variation of spring and fall field intensity with cosine of sun's zenith distance at Rose Polytechnic Institute (609 N. miles)

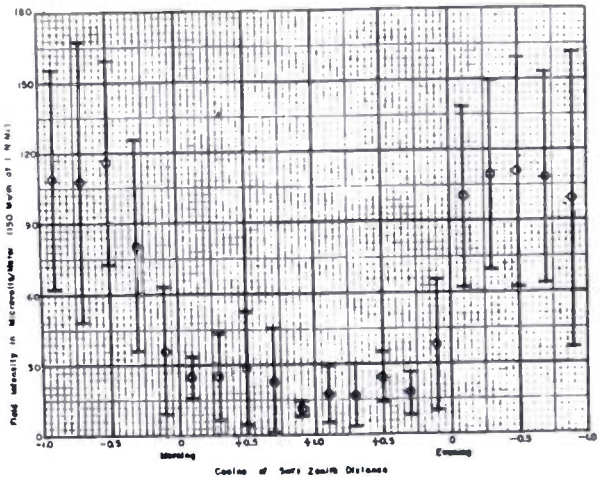

Fig. 10
Variation of spring and fall field intensity with cosine of sun's zenith distance at Parsons College (796 N. miles)

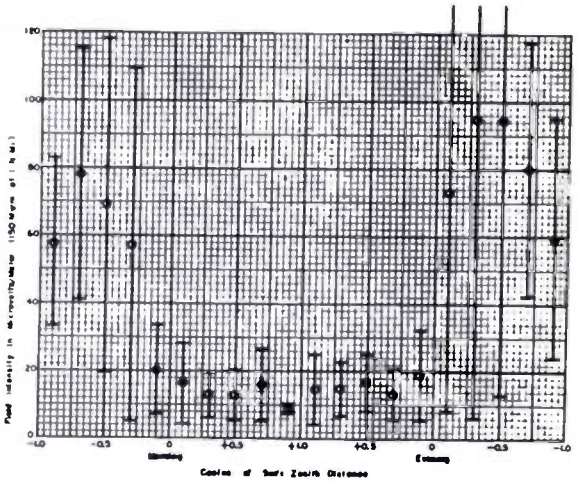

Fig. 11
Variation of spring and fall field intensity with cosine of sun's zenith distance at Hastings College (1,107 N. miles)

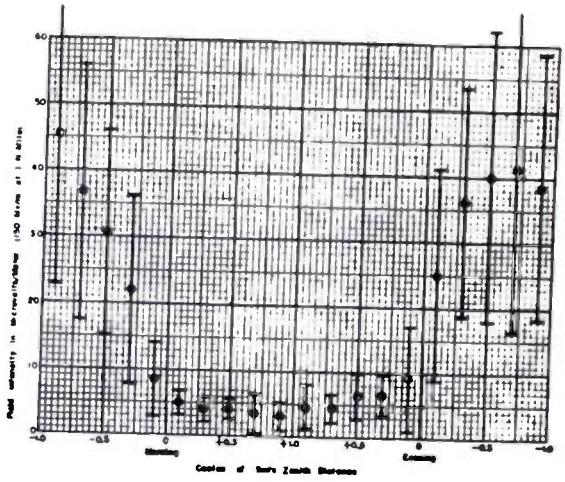

Fig. 12
Variation of spring and fall field intensity with cosine of sun's zenith distance at University of Colorado (1,424 N. miles)

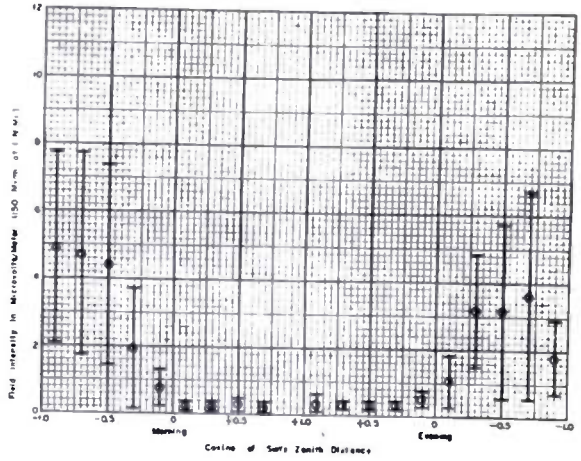

Fig. 13
Variation of spring and fall field intensity with cosine of sun's zenith distance at Stanford University (2,224 N. miles)

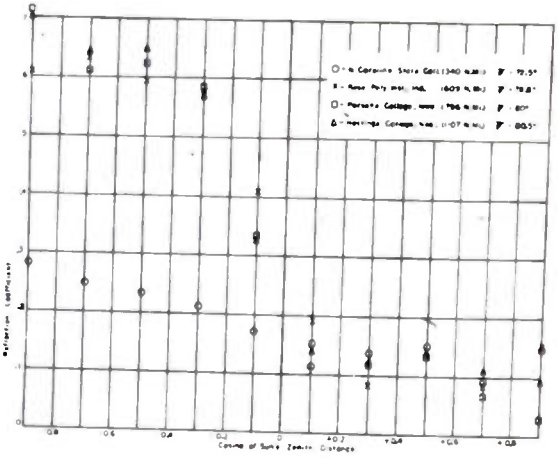

Fig. 14
Variation of reflection coefficient with cosine of sun's zenith distance and angle of incidence - ψ

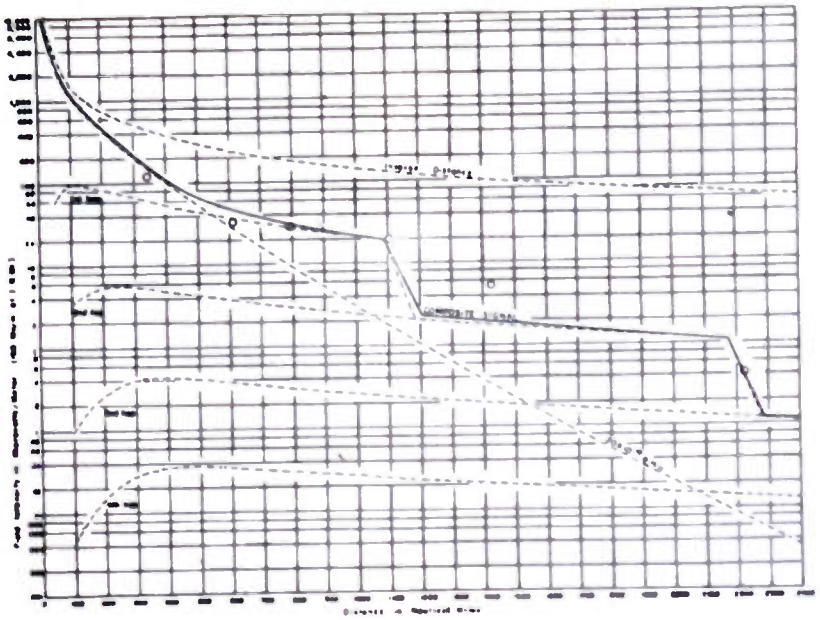

Fig. 15

Comparison of observed daytime field intensities with theoretical ground-wave and empirical sky-wave field intensities

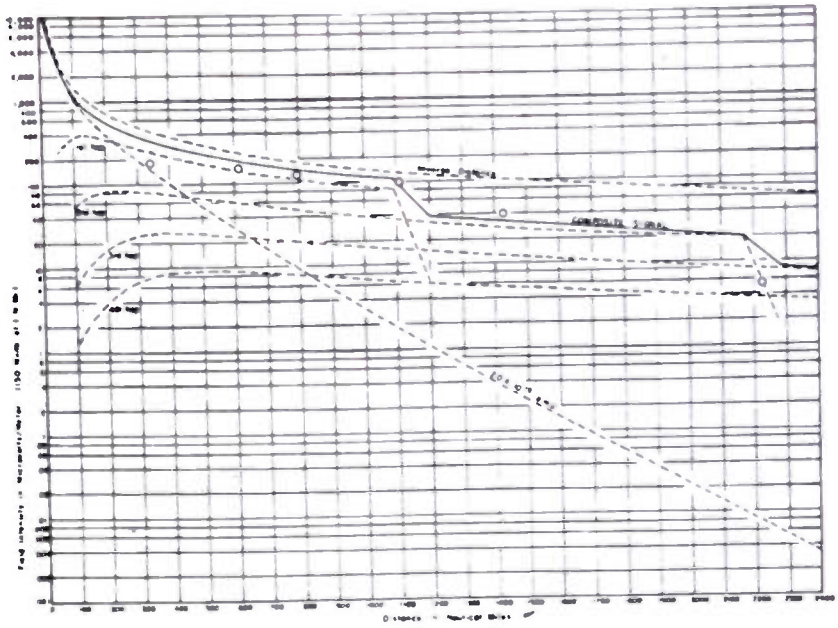

Fig. 16

Comparison of observed nighttime field intensities with ground- wave and empirical sky-wave field intensities

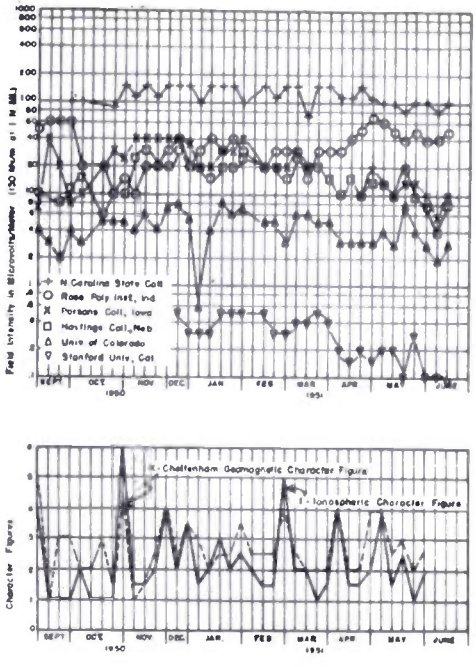

Fig. 17

Variation of daytime field intensity from week to week

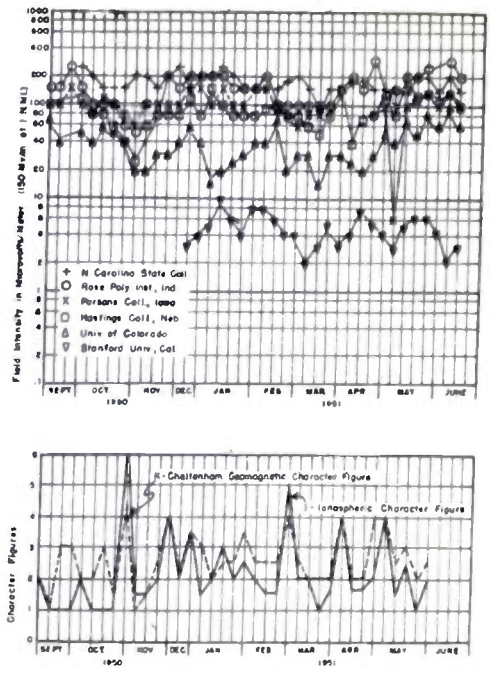

Fig. 18

Variation of nighttime field intensity from week to week

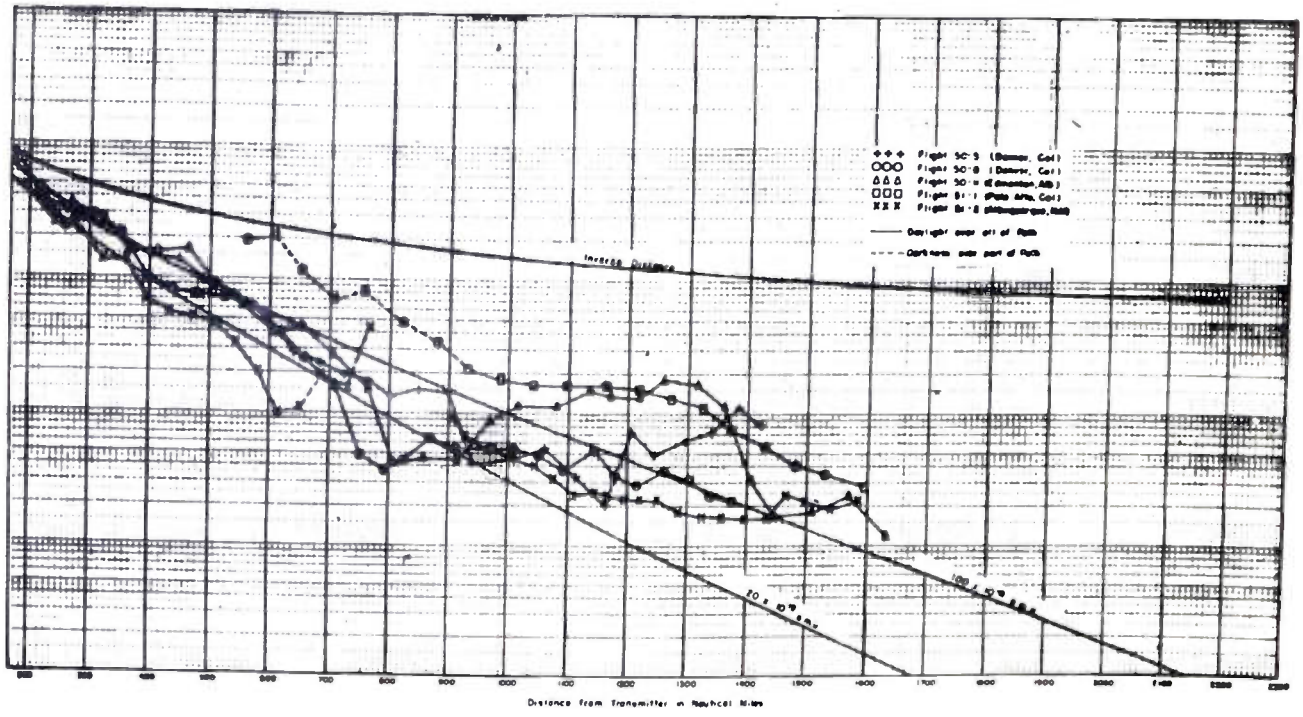

Fig. 19 - Summary of long-range day flights over land

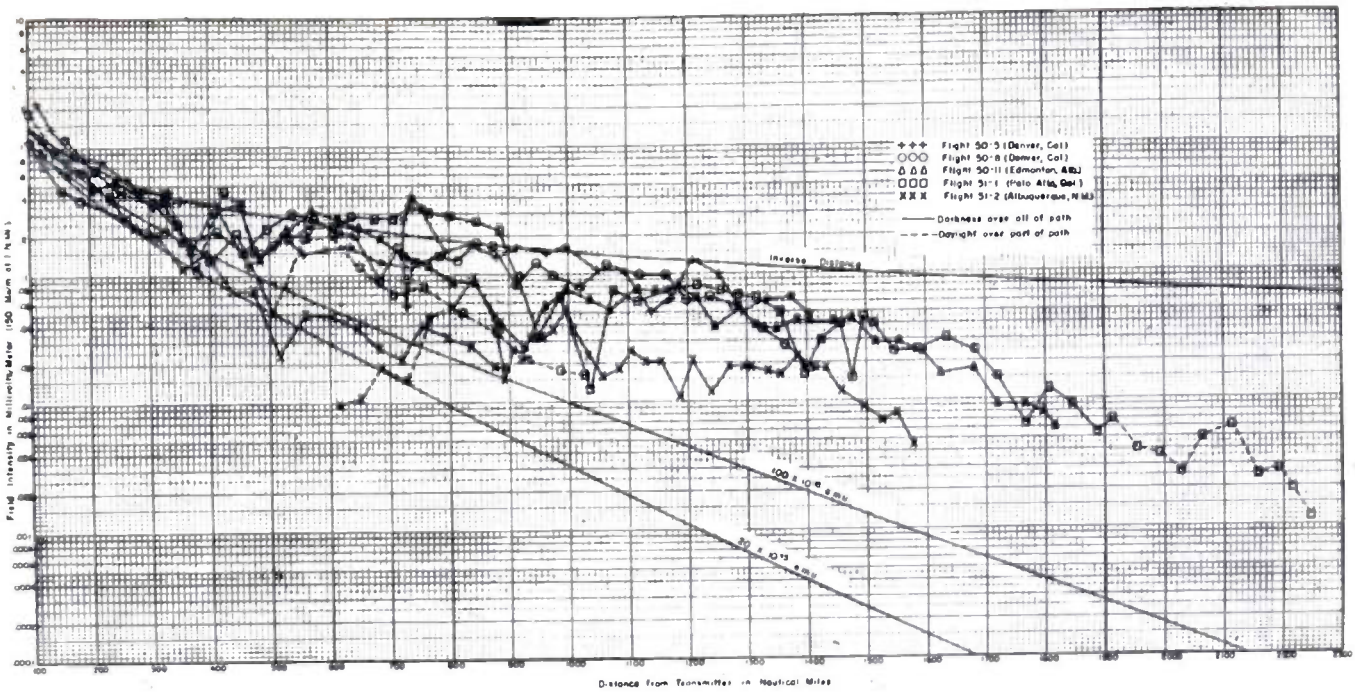

Fig. 20 - Summary of long-range night flights over land

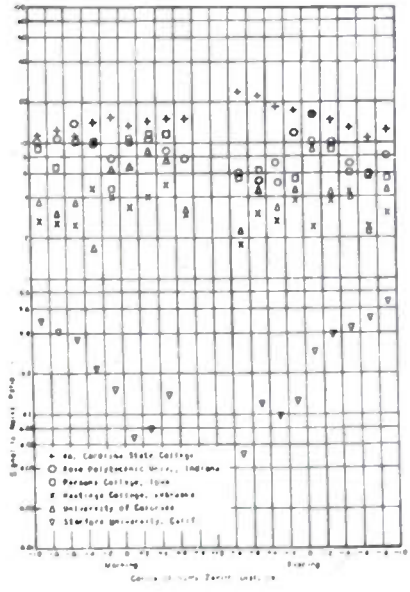

Fig. 21
Variation of winter signal-to-noise ratio with cosine of sun's zenith distance at ground monitor stations

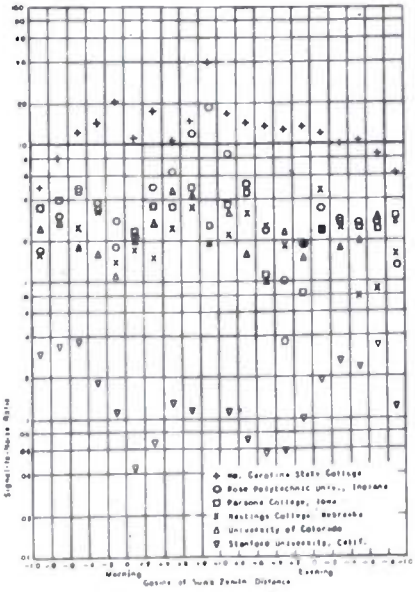

Fig. 22
Variation of spring and fall signal-to-noise ratio with cosine of sun's zenith distance at ground monitor stations

THE EFFECT OF SPORADIC E ON TELEVISION RECEPTION *

Ernest K. Smith
National Bureau of Standards
Washington, D.C.

For several years now reports of long distance reception have been coming in from television viewers. Most frequently these receptions have spanned distances of around 1,000 miles. There has been considerable speculation as to whether these anomalous receptions were tropospheric in origin or transmitted via the sporadic-E region of the ionosphere. A consideration is made here of the type of evidence leading one to conclude that transmission paths up to 500 miles can, roughly speaking, be attributed to tropospheric propagation, while sporadic E accounts for those transmissions of between 500 and about 1,600 miles. The importance of these receptions to television service in the United States lies not so much in the service gained through the long distance receptions themselves, but in the possible interference to a station's fringe area from distant co-channel stations.

To itemize some of the differences expected to be found between tropospheric and sporadic-E transmission, it may be noted first that skip distance does not apply to tropospheric propagation, while it does apply to sporadic-E. In terms of frequency, tropospheric phenomena will be more influential as frequency increases, while the sporadic-E reflections will, of course, decrease with increasing frequency. In terms of transmission distance, it may be expected that signals supported by the troposphere will decrease with path length, whereas those due to sporadic E will be most numerous at distances of around 1,000 miles. This last value is reached through consideration of the fact that although the skip distance curve would give us an increasing number of possible receptions up to the maximum distance for single-hop propagation, transmitting and receiving antenna radiation nulls for 0^{o} elevation have an opposite effect. Extraordinary tropospheric propagation over long paths must necessarily be dependent on conditions obtaining over a large extent of the path, whereas sporadic-E transmission would depend on the ionospheric conditions over the path midpoint only. As

---

* Research performed at Cornell University

sporadic E can be a highly localized phenomenon, if midpoints for a short time interval form a tight cluster on a map, sporadic-E rather than tropospheric propagation is indicated. Further evidence that sporadic E is responsible for anomalous receptions is obtained when reception midpoints are found falling close to the location of an ionosphere sounding station and when, at the time of the television receptions, sporadic E is identified on the ionosphere sounder.

The data utilized in this study were taken from the file of listener reports of Radio Electronics magazine.

These data contained 456 reports of receptions of stations on the various TV channels over distances greater than 200 miles. These reports were submitted by 103 persons and covered the period from May 22 to September 25, 1950. The crosses on Fig. 1 mark the locations of the observers. Cities with operating television stations are shown by circles. The channel numbers of operating television stations are shown for each city.

Shown in Fig. 2 is a histogram of the number of reports falling in the various class intervals of distance. The vast majority of reports is seen to fall in the 500- to 1,600-mile grouping and to consist almost wholly of receptions of low band (54- to 88-mc) stations. In the 200- to 500-mile range it may be noted that there are receptions of high band (174- to 216-mc) as well as of low band stations, and that there is a decrease with distance such that reports on both bands are negligible by 500 miles. This shows a rather sharp division between one group of reports in which the transmission distance was less than 500 miles and the other group with distances greater than this value. The former group is believed to be troposphere-propagated, whereas sporadic E could be responsible for the latter.

When the number of reports in the two distance divisions noted are plotted by channel as shown in Fig. 3, two difficulties arise. In the 200- to 500-mile grouping at the top, the number of reports appears to decrease with increasing channel frequency. The reverse would be expected for tropospheric transmission. In the 500- to 1,600-mile grouping, channel 4 rather than channel 2 received the greatest number of reports. However, there are more stations on channel 4 than on any other channel, and also more low-band than high-band stations. If the number of reports for each channel is prorated by the number of stations operating on the channel,

the distributions seen in the two lower charts are obtained. The high-band values now exceed the low-band ones for the 200- to 500-mile range as would be expected for tropospheric transmission, and the values decrease with channel frequency in the 500- to 1,600-mile range as would be expected for sporadic E[1].

In Fig. 4 is seen a chart of the number of reports per day for the period. The low-band reports are plotted in the upper histogram; the few high-band reports in the lower one. The number of hours of vertical incidence sporadic-E reflections at Washington, D.C. obtained at frequencies above 5- and 10-mc is shown in the center histogram. As the separation of the average midpoint from the Washington, D.C. ionosphere sounder is almost 1,000 miles, the day-by-day correlation between low-band reports and sporadic-E is about as good as could be expected. On a monthly basis, however, it should be noted that the greatest numbers of low-band reports occur in the months of June and July. These are also the months of greatest incidence of sporadic E over Washington, D.C.

It will be noticed that there are several days of exceptionally large number of low-band reports. July 16, in particular, has 40 reports. It is seen in Fig. 5 that on July 16 the midpoints form a dense cluster between Lake Michigan and Lake Erie. This looks like a sporadic-E cloud of the type reported by Ferrell and Gerson[2]. It is interesting to note that the cloud appears to have persisted for about four days from July 15 through July 18. This period was by far the most striking of any found, however, and is shown here as a sample of what can happen.

Shown on the upper map in Fig. 6 are points representing the locus of all possible midpoints between the 103 observers and the television station cities. The circles on the two maps represent the locations of ionosphere sounding stations from which overhead sporadic-E data might be available. The five U.S. stations reported in the CRPL F series -- Boston, Washington, Baton Rouge, White Sands, and San Francisco -- are seen to lie along the periphery of the country, and are therefore not ideally placed for propinquity with transmission-path midpoints. In map (b) (Fig. 6) the midpoints of the reported receptions are presented, and a somewhat southwesterly shift of center of mass of the points compared to the theoretical distribution above may be noted. Also there seems to be a certain number of the midpoints located close

to the Washington ionosphere sounder. Upon examination, four of these are found to fall upon the same day, June 27.

The location of these four midpoints is shown in (a) of Fig. 7 with the location of the ionosphere station at Washington. In (b) of Fig. 7 is a plot of sporadic E recorded at Washington, D.C. (solid curve) along with the occurence times for the midpoints plotted at their equivalent vertical critical frequencies. The coincidence is seen to be rather striking.

To summarize the findings, then, it is seen by the distribution of reception reports by distance that two distinct types of propagation are indicated for transmissions greater than 200 miles. One type seems to disappear at around 500 miles, which happens to be the point at which the other type becomes noticeable. This second grouping contains about 90 per cent of reports over 200 miles. When plotted as number of reception reports per station operating on the channel, the distribution by channel shows a predominance in the high band for the 500- to 1,600-mile group as would be expected for sporadic E. When compared to sporadic E at Washington, D.C. on a day-to-day basis, the low-band reports and sporadic E were seen to have similar seasonal distribution. Not so the high-band reports, which is as expected as they appear, with a single exception, in the 200- to 500-mile group. The path midpoints of the day for which the maximum number of receptions were reported are seen to form a tight cluster as they would if reflected from a slowly moving sporadic-E cloud. A coincidence test for a day when four of the reception paths over 500 miles in length resulted in midpoints near Washington, D.C. showed excellent simultaneity with observed sporadic E in three of the four cases.

With the hope that sufficient evidence has been presented to show that the 500- to 1,600-mile grouping is essentially sporadic-E propagated, a brief look at sporadic-E distribution as determined from ionosphere sounding stations will now be taken.

"Intense sporadic E" as used in Fig. 8 is defined as that producing vertical incidence reflections at frequencies above 7mc, this value being chosen because it is the highest one for which data are available in any quantity. The five locations are those listed above. It is noticeable that although considerable variation in shape and level exists among the stations, the well-known features such as the dominant June-July maximum and the March minimum are distinguishable in al-

most all the cases.

In order to increase the size of the sample and also to get a more generally representative distribution for the United States, the ordinate values for the five locations for each month are summed up.

The resulting chart, Fig. 9, is considerably smoother and more systematic in its trends. The summer peak shows a steady climb during the three years shown. This fits in rather well with the theory of inverse relationship of sporadic E with sunspot cycle[3]. As the next sunspot minimum is not expected until 1954 or 1955, it may be expected that sporadic E will increase for the next two summers at the same rate. This past summer's data, which have just been analyzed, indicate a peak of some 400 hours for June, 1951.

The diurnal curve shown in Fig. 10 was constructed from the data for five stations in the same manner as the seasonal distribution chart. The general form is very similar to that found by Mimno[4] in 1937.

References

1. For a similar chart see E.P. Tilton, Radio Electronics, vol. 22, p. 28; May, 1951.

2. O.P. Ferrell, Proc. I.R.E., vol 35, p. 493; 1947; vol. 36, p. 879; 1948.

   N.C. Gerson, Nature, vol. 116, p. 316; August 19, 1950; Proc. Conf. Ionosph. Phys., Pennsylvania State College, vol. 2, p. 200C; 1950.

3. M.L. Phillips, Trans. Amer. Geophys. Union, vol. 28, p. 71; 1947.

4. H.R. Mimno, Rev. Mod. Phys., vol.9, p. 1; 1937.

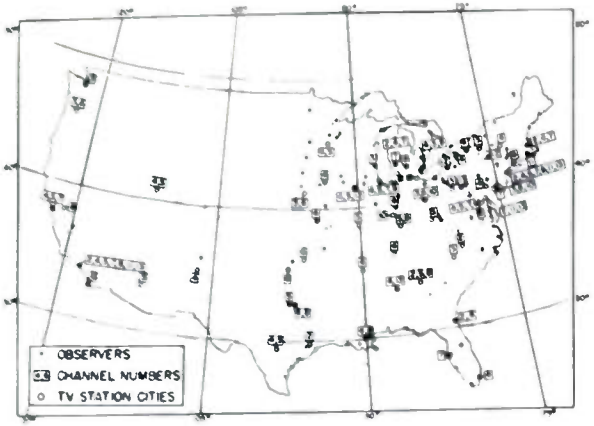

Fig. 1

Location of TV stations and observers

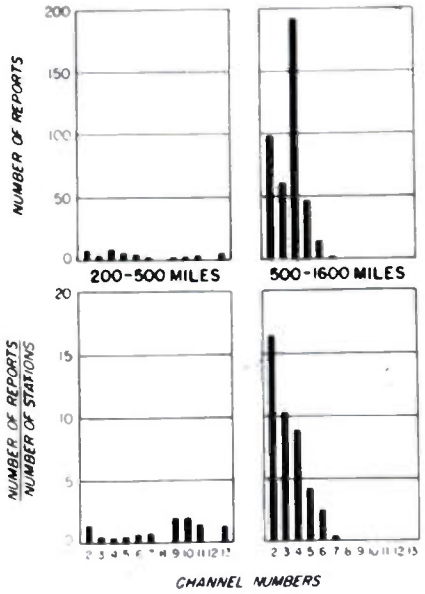

Fig. 3

Distribution of reports by channel: first for the total numbers of reports; second for reports per station

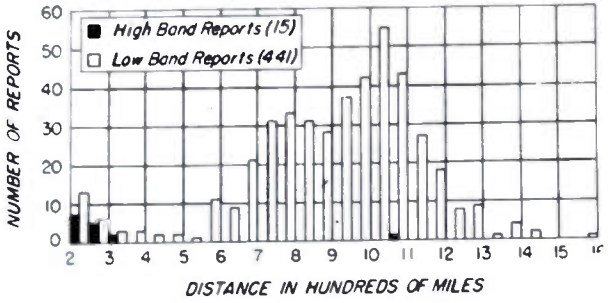

Fig. 2

Histogram of the distribution of television reports by transmission distance

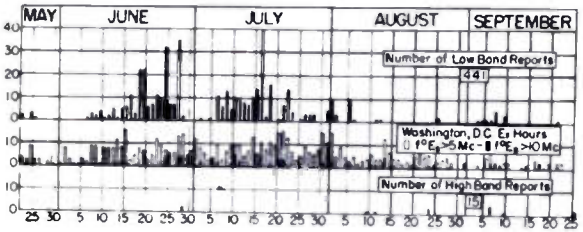

Fig. 4
Occurence of TV DX reports vs. occurrence of sporadic E

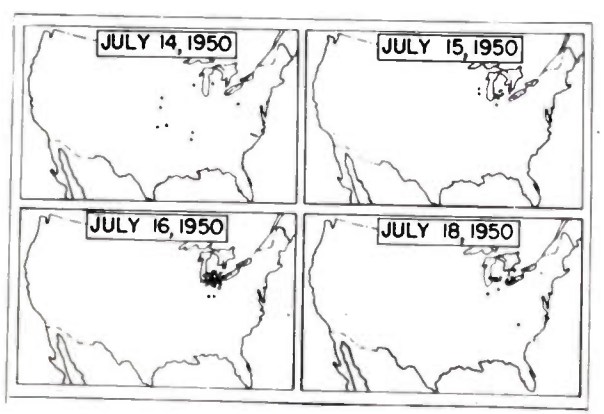

Fig. 5
Transmission path midpoints

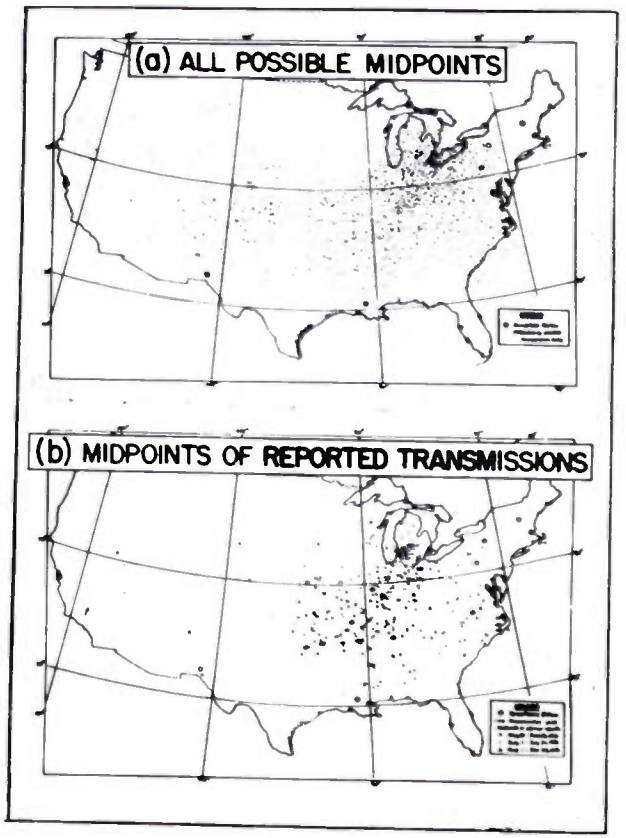

Fig. 6
Bias map showing (a) all possible midpoints and (b) midpoints of reported transmissions

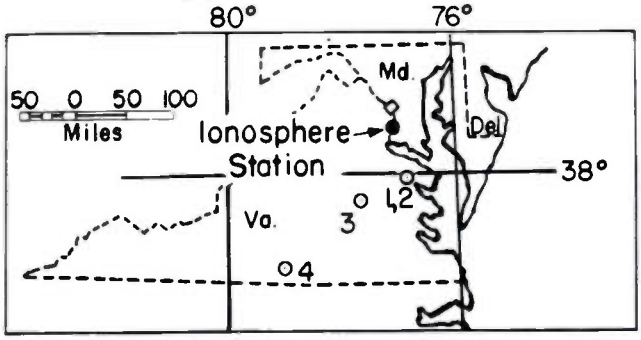

(a) Midpoints relative to sounder

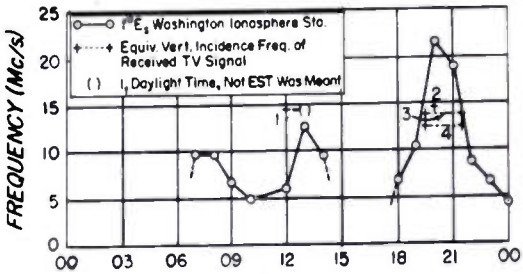

(b) Coincidence of TV receptions with sporadic E, June 27, 1950

Fig. 7 - Illustration of coincidence between reported sporadic E and long distance transmissions - June 27, 1950

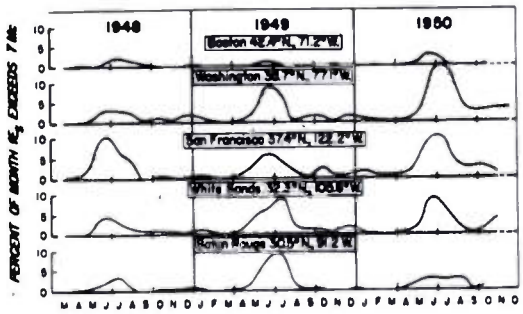

Fig. 8
Intense sporadic E at 5 U.S. stations

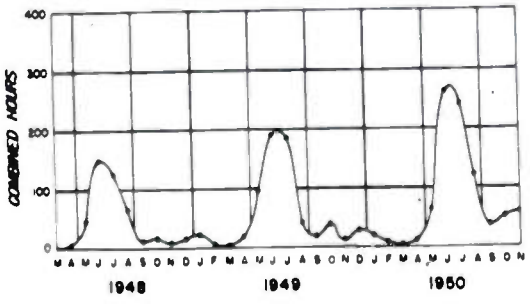

Fig. 9
Intense sporadic E.
Composite of 5 U.S. stations

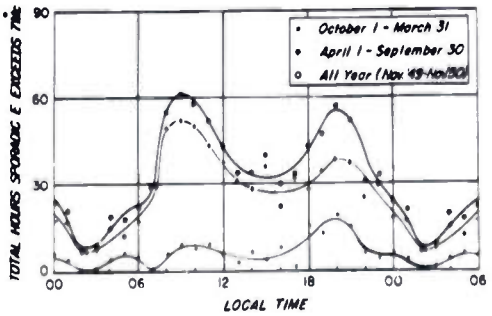

Fig. 10
Diurnal curve at intense sporadic E,
5 U.S. stations

A STUDY OF WINDS IN THE IONOSPHERE BY RADIO METHODS

J.H. Chapman
Canadian Defense Research Board

Winds in the ionosphere have been studied by a method due to S.N. Mitra using the fading of radio echoes at spaced receivers (Proc. IEE, London, 111, 43, p. 441; 1949). A mean daily wind variation of nearly semi-diurnal period and about 40 meters per second amplitude has been observed at a nominal height of 110 km (Region E). The wind variation is consistent with the explanation that it is due to tidal oscillations of the atmosphere. A wind variation consistent with that expected from lunar atmospheric tides has also been detected at this level.

The winds in the F region appear to increase in velocity with an increase in magnetic activity. A similar effect is not observed in the E region except during severe ionospheric disturbances.

(Abstract)

ON THE QUESTION OF THE MAGNITUDE OF THE LUNAR VARIATION IN RADIO FIELD STRENGTH

T.N. Gautier, M.B. Harrington, and R.W. Knecht
Central Radio Propagation Laboratory

Eight years of continuous recordings of the field strength of station WLW, and nine years of recordings of station W8XAL, both located near Cincinnati, Ohio, were examined for a lunar variation. The recordings were made at Washington, D.C. approximately 600 km away. The transmitted frequencies were 700 and 6080 kc, respectively. In the case of WLW, nighttime values of hourly median field strength were used. In the case of W8XAL, midday values were used. In neither case was the amplitude of the lunar semi-diurnal harmonic obtained by the analysis significantly greater than the probable error. The probable error in each case was approximately 0.3 db.

(Abstract)

THE LOWER E AND D REGIONS OF THE IONOSPHERE AS DEDUCED FROM LONG WAVE MEASUREMENTS*

J.J. Gibbons, H.J. Nearhoof, R.J. Mertney, and A.H. Waynick
Pennsylvania State College
State College, Pennsylvania

A diurnal and seasonal model representing the E and D regions of the ionosphere above State College, Pennsylvania is presented. This model consists of a Chapman-like E-region and an electron D-region. Approximate 150-kc wave solutions including coupling are obtained for this model. These wave solutions, of course, exhibit the well known reflection condition corresponding to an N value of around 3,000 electrons per cm^3. It is shown that the effect of the coupling is to cause a wave traversing a coupling region to excite a new wave propagated in the direction of propagation of the incident wave and also a back scattered wave propagated in the reverse direction. The back scattered wave will appear as a reflected wave originating in the coupling region. The forward scattered wave due to the downgoing wave from the upper "reflection" level also must be considered in calculating the polarization of ionospherically reflected waves.

It is shown that, in the case of 150-kc waves, the coupling effects occur in the neighborhood of $N \simeq 300$ electrons per cm^3, which corresponds to the "classical reflection" level for the "ordinary" wave. The coupling effects become greater as the ν associated with the coupling N value decreases toward $\nu = \nu_c$ for the nighttime models. This results in stronger split echoes and greater departure from circularity in the polarization ellipses.

The effect of the D-region is to introduce absorption and phase delay on the "ordinary" and "extra-ordinary" waves traversing it.

It is shown that the differences in phase path and absorption experienced by the ordinary and extraordinary waves give us two additional parameters with which to deduce the properties of the D-region, since it is these differences which help to determine the polarization of the down-coming wave. The experimental results to be expected from this model are compared in detail with our 150-kc polarization, absorption, and height results. The predicted experimental results are compared qualitatively with the actual experimental results at several other frequencies.

(Abstract)

* The research reported in this paper has been sponsored by the Geophysical Research Division of Air Force Cambridge Research Center under Contract AF19(122)-44.